# ADAPTIVE AND STEERABLE SATELLITE MULTIBEAM ANTENNA

Concluding report on Contract OSU77-00305

between

The Department of Electrical Engineering
Laval University, Quebec, Canada G1K 7P4

and

The Communication Research Center
Ottawa, Ontario

by

Jules A. Cummins, Gilles Y. Delisle and Marcel G. Pelletier

Electrical Engineering Department
Laval University
Quebec, Canada G1K 7P4



February 1979

ADAPTIVE AND STEERABLE

SATELLITE MULTIBEAM ANTENNA

Concluding report on Contract OSU77-00305

between

The Department of Electrical Engineering
Laval University, Quebec, Canada G1K 7P4

and

The Communication Research Center
Ottawa, Ontario

by

Jules A. Cummins, Gilles Y. Delisle and Marcel G. Pelletier

Electrical Engineering Department
Laval University
Quebec, Canada G1K 7P4





February 1979

ACKNOWLEDGMENT

The authors wish to express their gratitude to the following members of the Department of Electrical Engineering at Laval University for their respective contributions to the work described in this report:

Mr. Guy Morin, Designer,
Mr. Phieu Le-Huy, Research Assistant,
Mr. Gilles Bisson, Technician,
Mr. Gaston Guay, Draftman.

They are also extremely grateful to Dr. A.K.C. Kong for his services as Scientific Authority for the Department of Communications on this contract.

TABLE of CONTENTS

## SUMMARY OF THE REPORT

An outline is presented of the fundamental theory underlying a method of discriminating against interference in satellite communications by using an adaptive algorithm operating in real time on the received signals of an antenna array. A brief description is given of the design considerations and of the system analysis that motivated our choice of the basic circuitry upon which satisfactory performance of the system is dependent. The main topic discussed in that section of the report is the closed loop circuit controlling the adjustments of the weights given to the array outputs as they are scanned sequentially. Also included is a schematic of the somewhat complex hybrid computer program prepared for simulating, in scaled time, the operation of a two-element array illuminated by the signal from broadside while interference is incident upon it from various directions. This part of the report contains numerous novel computer software techniques that had to be developed before any attempt could be made at simulating the system's operation.

## 1. INTRODUCTION

Since the publication in 1967 of the now classic paper by Widrow and his co-workers, on adaptive array antenna systems [1], the various methods that were proposed for processing antenna signals adaptively have aroused an ever increasing interest [2,3]. The feature that makes these antennas so attractive is their ability to sense, automatically, an interference environment and minimize its effects by steering nulls or by reducing sidelobes in the direction of the interference.

In applications involving telecommunications, a variety of methods may be used for controlling the array weights. The best known are the gradient technique implemented with a least-mean-square (LMS) algorithm [4] and the sample matrix inversion technique [5]. The technique that we propose is a form of the gradient technique implemented through the repeated use of a servomechanism loop of the "on-off" type.

## 2. PURPOSE OF THE PROJECT

The long term objective of the project is to analyse and design a signal processing unit for a multilobe receiving antenna having the following capabilities:

a) that of discriminating between desired and interfering signals, for example by using a beacon or pilot signal;

b) that of adjusting the weights (i.e. amplitude and phase) of the signals from each antenna element in an automatic fashion and in such a way as to maximize the S/N ratio in spite of changing conditions in the signal or in the interference.

## 3. METHOD OF APPROACH

The schematic diagram originally submitted in the proposal is only one of several possible methods by which the "on-off" adaptive technique could be implemented. An alternate method is shown in Fig. 1 in

which the weights are applied to the array signals at I.F. frequencies instead of R.F.

The distinctive characteristics of the proposed system are listed below:

a) a portion of the transmitted signal is used for identifying its direction of arrival;

b) the weighting given to the output of each element in the array is implemented by means of electronically controlled phase shifters and by electronically controlled attenuators. The latter could be replaced by variable gain amplifiers;

c) the weights are adjusted sequentially;

d) the servo-loops are of the type designated as "on-off" in servomechanism literature (plus-ou-moins, the term used in the French literature on automatic control seems more appropriate);

e) the system can be used either with multibeam antennas or with arrays of highly directive antennas.

## 3.1 Principle of Operation.

The parameter to be optimized is the S/N ratio which bears a direct relation to the weights. However, the servo-loop uses the time derivative of S/N to perform the optimization. This can be understood by considering the properties of the adaptive algorithm as described in the following section.

## 3.2 Adaptive Algorithm.

Let $W_i = w_i e^{j\phi_i}$ be the complex weight associated with the $i^{th}$ antenna element, where $w_i$ is the amplitude and $\phi_i$ the phase of $W_i$.

The variation $\Delta(S/N)$ of the S/N ratio depends on the weights and, for the $i^{th}$ weight, may be expressed as follows:

$$\Delta(S/N) = \frac{\partial(S/N)}{\partial w_i} \Delta w_i + \frac{\partial(S/N)}{\partial \phi_i} \Delta\phi_i \qquad (1)$$

We may consider the S/N at the output of the summer as a functional of a

vector V consisting of the 2n components of the weights, that is

$$V = (w_1, w_2, \ldots, w_n, \phi_1, \phi_2, \ldots, \phi_n) \quad .$$

It has been shown [6] that the fastest increase in S/N is in the direction defined by the following gradient:

$$\nabla(S/N) = \left[\frac{\partial(S/N)}{\partial w_1} \cdots \frac{\partial(S/N)}{\partial w_n}, \frac{\partial(S/N)}{\partial \phi_1} \cdots \frac{\partial(S/N)}{\partial \phi_n}\right] \tag{2}$$

Eq. (2) implies that the increase in S/N can be made gradually.

If the increase in (S/N) is achieved one step at a time, then the weights at step $(1+n)$ are related to those at the previous step n as indicated below:

$$w_i^{(n+1)} = w_i^{(n)} + \alpha \frac{\partial(S/N)}{\partial w_i} \tag{3}$$

and

$$\phi_i^{(n+1)} = \phi_i^{(n)} + \beta \frac{\partial(S/N)}{\partial \phi_i} \tag{4}$$

where $\alpha$ and $\beta$ are small positive real constants. The parameters $\alpha$ and $\beta$ must be sufficiently small for stability, but strong enough for reasonably rapid convergence.

In the system that we propose the change in the weights is to be made sequentially by switching. In eq. (2), the derivation of (S/N) is taken with respect to $w_i$ or $\phi_i$, but the time derivative of S/N can also be used as a criterion for determining how the weights are to be changed at each step.

Assuming that a small change takes place in $w_i$, the first order change in (S/N) is:

$$\Delta(S/N) = \frac{\partial(S/N)}{\partial w_i} \Delta w_i \tag{5}$$

which is equal to:

$$\Delta(S/N) = \frac{\partial(S/N)}{\partial t} \cdot \frac{\partial t}{\partial w_i} \nabla w_i \tag{6}$$

or equivalently,

$$\Delta(S/N) = \frac{\partial(S/N)}{\partial t} \cdot \frac{\Delta w_i}{\frac{\partial w_i}{\partial t}} \tag{7}$$

Because the quantity $\Delta w_i/(\partial w_i/\partial t)$ is always positive, eq. (7) may be rewritten as follows:

$$\Delta(S/N) = \frac{\partial(S/N)}{\partial t} \cdot k\left|\Delta w_i\right| \tag{8}$$

where $k$ is a positive constant.

Eq. (8) implies that $\partial(S/N)/\partial t$ must be positive for the S/N ratio to increase. Therefore our task is to find the sign of $\Delta w_i$ which will make $\partial(S/N)/\partial t$ positive.

The above reasoning is quite similar to the logic underlying the operation of the "on-off" type of servomechanisms. Expressed in simple terms, this logic is equivalent to the following statement: "If a change in the control improves the desired output, the sign for the next change must be kept the same as it was in the previous one, otherwise it must be reversed".

## 3.3 Control Law in the "On-off" Type of Servomechanism.

Fig. 2a [7] shows the schematic diagram of a single loop servomechanism with time derivative control. In this class of servomechanisms, the control system uses the error $dy/dt$ to perform a $dx/dt$ command on the process. For the "on-off" type, the control law is generally such that it can be expressed by the following equation:

$$\frac{dx}{dt} = \kappa \text{ sign } \frac{dy/dt}{dx/dt} = \kappa \text{ sign } \varepsilon \tag{9}$$

where $\kappa$ is a positive constant and sign $\varepsilon$ means the sign of $\frac{dy/dt}{dx/dt}$.

It is apparent from eq. (9) that the absolute value of the command signal $dx/dt$ does not depend on the error signal $dy/dt$. In the search for a maximum value of $y$ (which corresponds to S/N in our case), eq. (9) may be interpreted to mean the following: "As long as $dy/dt$ is positive, the sign of the control signal must remain unchanged; if $dy/dt$ becomes negative, the sign of the control signal must be reversed except when $dy/dt$ changes from a negative to a positive value.

## 3.4 Typical Response of "On-off" Servomechanisms.

The typical response of an "on-off" servomechanism is illustrated in Fig. 3a [8]. It can be seen that permanent oscillations are present. These oscillations are inherent to the limited time response of the system. An increase of the oscillation frequency will in general reduce the amplitude of the oscillations. A design goal is evidently to reduce the amplitude of the oscillations as much as possible. For example, if a delay in response or hysteresis (caused by the limited sensitivity of the comparators) occur in commutation, then the amplitude of the oscillations increase as shown in Fig. 3b. Oscillations could be completely nulled [8] by the use of idle times in the control signal as indicated in Fig. 4. However, a price must be paid in the form of a decreased precision (lower S/N).

## 3.5 Dynamics of the Process.

In addition to the delay due to commutation, limited time response also occurs in

a) the detection of the error signal (the change in S/N is not instantaneously detected);

b) the process itself (the response to the control signal is not instantaneous).

This is schematically illustrated by the addition of transfer functions boxes in the loop as shown in Fig. 2b.

The time response of the weights to the control signals has been measured as explained in appendix A. This time constant of the response is about 2 μs for the phase shifters and 3 μs for the attenuators.

### 3.5.1 Dynamics of the Error Signal Detection:

The system will converge to the optimum solution unless drifts are present in the characteristics of the process [7]. These drifts can be interpreted as changes in the position of the signal source or of the interference.

### 3.5.2 Dynamics of the Process Itself:

If the relation between V and X (Fig. 2b) is linear and may be represented by the following Laplace transform:

$$F_1(P) = \frac{X(P)}{V(P)} = \frac{1}{1+\tau P} \quad , \tag{10}$$

it can be shown that the system is stable if

$$|X - V| < |\kappa\tau| \quad \text{at} \quad t = 0$$

with $$\kappa = \pm \left|\frac{dx}{dt}\right| \quad .$$

Now if V is a ramp signal (this is our case) $|X - V|$ is never greater than $|\kappa\tau|$ and the system remains stable.

## 3.6 Adaptive System Convergence.

The weights are adjusted sequentially, one at a time, and each adjustment depends upon the values that all other weights have at that instant. Under those circumstances, it may not be immediately evident that the system will always converge to the optimum signal-to-noise ratio (S/N). Situations are conceivable, for instance, such as those illustrated in Fig. 6b, in which a system would settle at a different local maximum depending upon its initial state.

This section will show that such situations will not occur, because the S/N as a function of the weights has a unique maximum (Fig. 6a) thus ensuring convergence of the adaptive system.

### 3.6.1 Formulation of the Signal-to-Noise Ratio:

An expression for the signal-to-noise ratio (S/N) will be derived under the following assumptions:

a) weighting is realized by power distribution rather than by dissipation in resistive elements;

b) both signal and interference are assumed to occupy an extremely small portion of the frequency spectrum;

c) for simplicity, interference will be the only form of external noise included in the formulation.

Let $w_i$ be the complex weight associated with the $i^{th}$ antenna element and $v_i$, the complex signal appearing at the terminals of the same antenna when an external signal source is transmitting from direction $(\theta_1, \phi_1)$. Then, the signal power, S, at the receiver may be expressed as:

$$S = Y_0 \left| (v_1 w_1 + v_2 w_2 + \ldots\ldots + v_n w_n) \right|^2 \tag{11}$$

where $Y_0$ is the characteristic impedance of the line.

Eq. (11) may be rewritten in matrix form:

$$S = Y_0 [w^*][v^*][v][w] = Y_0 \langle w|V|w\rangle \tag{12}$$

where $|V| = [v^*][v]$ ,

$[v]$ being a row matrix,

and $[w]$ , a column matrix.

The shape of the radiation pattern is not altered if only the relative amplitudes of the $w_i$'s are considered. Moreover, whatever absolute value the $w_i$'s may assume, a normalization of S such that:

$$S = Y_0 \frac{[w^*][v^*][v][w]}{[w^*][w]} = Y_0 \frac{\langle w|V|w\rangle}{\langle w|w\rangle} \tag{13}$$

insures that S is exactly equal to the signal power at the output of an ideal passive weighting network.

Similarly, the power received from an interfering signal N of direction $(\theta_2, \phi_2)$ can be expressed as:

$$N_1 = \frac{Y_0 [w^*][j^*][j][w]}{[w^*][w]} = \frac{Y_0 \langle w|J|w\rangle}{\langle w|w\rangle} \tag{14}$$

in which $[j]$ and $|J|$ are, respectively, the row matrix and the full size matrix of the received interfering signals, in complex form.

If $N_2$ denotes the receiver noise, the S/N ratio of the complete system is given, in this case, by the following expression:

$$S/N = \frac{Y_0 \dfrac{\langle w|V|w\rangle}{\langle w|w\rangle}}{Y_0 \dfrac{\langle w|J|w\rangle}{\langle w|w\rangle} + N_2} \tag{15}$$

$$= \frac{\langle w|V|w\rangle}{\langle w|J|w\rangle + k\langle w|w\rangle} \quad , \quad k \text{ being a constant.} \tag{16}$$

Eq. (16) was derived for a single interfering source, but any number of these could be included in the formulation. It is possible to rewrite eq. (16) in a more compact form, as follows

$$S/N = \frac{\langle w|V|w\rangle}{\langle w|B|w\rangle} \tag{17}$$

where $|B| = [J] + k[U]$ ,

$[U]$ being the unitary matrix.

Thus, the expression for S/N reduces to a ratio of two quadratic forms that are positive definite, since S and N both represent power. Also, it should be mentioned that matrices [V] and [B] are Hermitian.

At the maximum of eq. (17) and at the secondary maxima of the same equation, if they exist, the following relations must hold:

$$\frac{\partial(S/N)}{\partial w_i} = 0 \qquad \text{and} \qquad \frac{\partial(S/N)}{\partial w_i^*} = 0 \tag{18}$$

for all i's. When these relations are applied to the (S/N) as expressed by eq. (17), there results the following eigenvalue equation [10]:

$$[V][w] = S/N[B][w] \tag{19}$$

The weights [w] satisfying (18) are the eigenvectors of (19) and the eigenvalues of the same equation are equal to the S/N ratio corresponding to this choice of the weights.

However, as was shown by Cheng and Tseng [11], all the eigenvalues of (19), except one, are equal to zero since [V] is a dyadic matrix. This proves that S/N, expressed as a function of the weights, has indeed a unique maximum.

## 4. STATUS

Since inception of the projet, work has progressed along parallel paths in three distinct areas that are interdependent:

a) the theoretical aspects of the adaptive algorithm underlying our method of approach;

b) the design of a laboratory prototype of the basic control loop;

c) a hybrid computer simulation of the system.

Area a) concerning the basic theory of the project was described in the preceding sections of this report. In this section a brief description is presented of the work done in areas b) and c) of the project.

## 4.1 Design of a Laboratory Prototype.

The implementation fo a single adaptive loop was the first objective of the experimental portion of the project and has been realized successfully. It can, therefore, be argued that feasibility has been demonstrated experimentally, because, in a sequential process such as the one that we use, only one loop is operational at a given time. Convergence for one loop is sufficient to demonstrate convergence for the complete adaptive process.

Fig. 5 shows a schematic diagram of the basic loop controlling a single phase shifter. In this figure, two antenna signals entering the lines in plane AB are simulated by a divider combiner arrangement. For simplicity, the magnitude of the interfering signal I is made equal on each line, so that a phase shifter ($\Phi_E$) is then sufficient to null the I component at the summer output without the use of an attenuator.

### 4.1.1 Processing used for Isolating the Pilot Signal:

The method used for filtering and isolating the pilot signal out of all the signals accepted by the antenna is achieved by using a phase locked loop (PLL) with AM detection. The PLL NE 561 B of Signetics is the component chosen for this task. Ideally, the pilot branch should isolate the pilot signal uniquely, but, unfortunately, this isolation is limited as shown in appendix B. The effects of this limitation will be analyzed in a follow-on contract.

The amplifier preceding the PLL serves a dual purpose: it insures a match to the input of the PLL at an optimum signal level. In order to monitor the total power in the frequency band, another IF amplifier of appropriate bandwidth (10% in this design) is followed by a power sensor.

The circuit design of these two adjustable gain IF amplifiers is shown in Fig. 7. Low frequency amplifiers are added in each branch to

bring the DC level at the output S to about one volt. A circuit extracting the square root is included in the $(S+N)$ branch, because the power sensor (HP 423 A) provides a DC voltage proportional to the input power whereas the PLL output is proportional to the input voltage.

4.1.2 Processing Used for Detecting the Error Signal:

The adaptive algorithm adopted for this system uses a nonlinear automatic control process. Consequently, the sign of $(d/dt)(S/N)$ is the only criterion considered by the process regardless of amplitude. Noting that $\frac{d}{dt}\left(\frac{S}{S+N}\right) = \frac{N^2}{(S+N)^2}\frac{d}{dt}(S/N)$, is sufficient to show that either $(d/dt)\left[S/(S+N)\right]$ or $(d/dt)(S/N)$ would give a valid criterion, since both have the same sign.

The process tested experimentally in the laboratory implements $(d/dt)\ S/(S+N)$ . The circuit used for performing that operation is shown in Fig. 13.

Control of the Weights:

The purpose of the control is to implement the logic of the "on-off" servomechanism. The control system is schematically illustrated in Fig. 16. Basically the system reverses the sign of the control signal (in front of the integrator) when the derivative of S/N is negative. More precisely, when a change from + to - is detected by the polarity detector, the bistable settles in a new state and the switch commutes.

Appendix C describes the signal processing circuits designed to implement the adaptive system.

4.2 Simulation Techniques.

The adaptive system proposed in this contract was simulated on a 690-EAI Hybrid Computing System for a dual purpose:

1) to establish firmly the soundness of the basic principles underlying the design and operation of the system;

2) to study the effects that the various parameters of the system will have upon its performance.

The second objective was realized only partly, because of limitations in the number of computer components available on the 690-EAI. For this reason, the simulation had to be restricted to the study of a two-element array and one automatic control loop for the continuous adjustment of one weight. Moreover, the computer was utilized to the limit of its speed capabilities; thus severe restrictions were imposed upon the choice of the time constants that could be studied with the computer.

The simulation diagram described in the preliminary report had to be revised, mainly for the following reasons:

1- In the simulation, preference had to be given to circuits requiring the smallest number of components for their operation. Even the simple case of a signal originating from broadside requires, in the simulation, that equal phase shifts be produced for the signal and for the noise, which implies that the weighting network must be duplicated. It was therefore important to design a type of phase shifter that uses a minimum number of components. The operating principle of this phase shifter is described in Annex I.

2- The ratio $S/S+N$ had to be computed in a different manner. In fact, the slowest derivative circuit that we were able to implement had a time response many times faster than the time constants of the filters that were first proposed to extract the signal from the remaining of the spectrum. For this reason, a new type of filter was selected which allowed unwanted transients to be eliminated, so they would not be detected by the derivative circuit.

3- Due to the limited capacity of the computer, the diagram, designed originally for the study of a four-element array with commutation, had to be modified and now simulates a two-element array without commutation.

The simulation diagram and the results of the simulation are given in Annex I. The work reported here has also been the subject of a contribution presented at the IEE International Conference on Antennas and Propagation held in London, England, 28-30 November 1978. The text of that presentation is included in Annex II.

## 5. RESULTS

The results of the theoretical analysis, the computer simulation and the experimental verification performed in the laboratory, all prove, beyond any doubt, the soundness and feasibility of the proposed adaptive system. Excellent agreement has been observed between the results of the computer simulation and the theoretical predictions. It has also been shown that the system will converge to the optimum value of signal-to-noise ratio provided that the environment does not change at a rate faster than the system can follow. Experimentation is still in progress with the laboratory system operating in real time, but enough is already known to demonstrate feasibility.

# Appendix A

## Time Response Measurement of the electronic phase shifters and attenuators

The time response of the electronic phase shifters must be measured indirectly, because no instrument is sufficiently rapid for a direct measurement. The schematic diagram of Fig. 8a shows how the properties of the hybrid junction were used to translate the phase information into a corresponding amplitude. For example, if the signals $A \cos \omega t$ and $A \cos (\omega t + \phi)$ are applied to the input ports of a $180^{\circ}$ hybrid junction, the output appearing at the $\Sigma$ port is $A \cos \frac{\phi}{2} \cos(\omega t + \frac{\phi}{2})$. The time response of the electronic phase shifter can then be measured by applying a voltage step to the phase shifter control input and by monitoring the output of the hybrid junction.

The voltage step is obtained from a square wave generator having a 5 ns risetime and a 10 $\Omega$ output impedance.

Fig. 9 shows the phase shifter control signal (bottom wave) and the signal appearing at the output of the bandpass filter. The purpose of the 30 MHz filter is to reject the low frequency components reaching the RF line through the control input of the phase shifter.

The measurement of the electronic attenuator time constant can be achieved with the apparatus shown in Fig. 8b. In this case, a current step is applied to the control input of the attenuator. The measurement of the time constant gives 2,4 μs when the current is applied and 3,6 μs when the current is turned off.

# Appendix B

## Filtration of the Pilot Signal

The filter for the pilot signal is built around Signetics' NE 561 B phase locked loop (PLL) and its schematic diagram is shown in Fig. 10. To explain how the circuit operates, let us assume that an IF signal is present at the input and the PLL is locked on it. Then a DC voltage proportional to the IF signal appears at the output. Ideally, the PLL bandwidth should be extremely small in order to detect the pilot signal uniquely. With the NE 561 B, the capture range and the lock range are as shown in Fig. 11. A narrower capture range could be obtained, but the temperature stability of the circuit would have to be increased, particularly at low IF levels.

This circuit has another disadvantage: its capture range is wider for inputs of higher level. Consequently, if an interfering signal stronger than the pilot signal were to appear at the input, the PLL would very likely lock on it, as is apparent from Fig. 11.

An important characteristic of the filter is the isolation between the pilot signal and the interfering noise. This has been measured for the case of an interfering sinusoïdal source. The results, presented in Fig. 12, indicate how the strength of an interfering source affects the pilot signal power appearing at the filter output.

The temperature stability of the circuit also affects the pilot signal power. For indoor operation of the filter, this effect has been measured and was found to be smaller than .02 V.

# Appendix C

## Signal Processing Circuitry for an Adaptive Antenna System

Fig. 1 shows a schematic diagram of the proposed adaptive array signal processing system. It consists of three main parts not including the weighting network. The first part isolates the pilot signal and measures the total received power (including noise) in the desired signal passband. This operation provides an estimate of the S/N ratio. The second part generates an error signal proportional to the time derivative of the system S/N. The third part implements the logic inherent to the operation of "on-off" types of servomechanism automatic control and provides the excitations that must be applied to the weighting network.

Fig. 5 shows the circuit diagram of an experimental type of servo control loop now under test. Isolation of the pilot signal and application of the weights to the received signals are both carried out at IF frequencies. The method used for separating the pilot signal from all the signals accepted by the antenna is based upon the operation of a phase-locked loop circuit followed by AM detection. The total power accepted in the signal passband appears in a branch distinct from the one containing the pilot signal and is measured with a crystal detector.

The output of the detected signals in each branch can be considered as slowly varying DC voltages which can be processed as such to produce the error signal. The circuits shown in Figs. 13, 14 and 15, implement, respectively, $\frac{d(S/S+N)}{dt}$, $\frac{d(S/N)}{dt}$ and $\left(N\frac{dS}{dt} - S\frac{dN}{dt}\right)$, which will also be experimented in a follow-on contract.

Figs. 16 and 17 illustrate schematically the method of system control. It consists, essentially, in providing a reversal of sign for the control signal, whenever the error signal, which is proportional to the derivative of S/N, is negative.

# Annexe I

par

Gilles Y. Delisle et Marcel Pelletier

A. DESCRIPTION DU DIAGRAMME DE SIMULATION.

B. RESULTATS DE LA SIMULATION.

# Annexe I

par

Gilles Y. Delisle et Marcel Pelletier

## A. DESCRIPTION DU DIAGRAMME DE SIMULATION

### Bloc # 1 Simulation du signal

Le premier point à considérer est que le signal pilote, qui est aussi le signal désiré, soit une sinusoïde de fréquence stable et d'amplitude constante. La simulation doit aussi fournir un mécanisme permettant de varier indépendamment l'amplitude et la phase du signal pilote. Ceci est particulièrement important si l'on veut éviter que la phase soit modifiée pendant un ajustement d'amplitude et vice-versa.

Selon le diagramme de simulation de la Fig. 18, le signal désiré est généré par un oscillateur harmonique dont la fréquence d'opération est 600 cycles. La sortie de cet oscillateur est reliée au comparateur C-1, dont l'une des entrées est à la terre. Cela remplit la fonction de détecteur de zéro et il apparaît évident que la sortie du comparateur est une onde carrée de même fréquence que l'oscillateur. Entre les périodes d'opération du calculateur, cette onde carrée est désactivée au moyen d'une porte logique et du signal d'horloge B. De fait, la durée de la période d'opération est contrôlée de façon externe puisque le contrôle interne du calculateur ne permettait pas d'obtenir des périodes d'opération suffisamment longues pour nos besoins.

L'onde carrée est alors réduite à une impulsion de 10 μs en la passant dans un différentiateur logique DF-1, lui-même suivi d'un monostable MS-1. Cette impulsion qui se produit à chaque cycle replace l'intégrateur I-3 à sa condition initiale de -.9 u.m. (unité machine). Le but de cet intégrateur est de produire une rampe répétitive symétrique par rapport à la terre et de même fréquence que l'oscillateur harmonique, i.e. 600 cycles. Ce signal se divise en deux parties qui sont reliées respectivement aux comparateurs C-2 et C-3. La portion du diagramme entre le comparateur C-2 et le sommateur A-15 simule effectivement la pondération du signal par l'antenne n° 2. Le déphasage est d'abord réalisé, au niveau logique, comme suit: Pour l'antenne n° 1, l'onde triangulaire est

d'abord comparée au niveau de contrôle, lequel provient de l'intégrateur I-3. La sortie du comparateur C-2 est une onde carrée logique dont le point de départ dépend du niveau de contrôle appliqué; c'est le principe du déphaseur variable puisqu'un délai égal à une période complète correspond à un déphasage de 360°. Cependant la sortie du comparateur C-2 est non symétrique, en ce sens qu'elle peut être plus longtemps dans l'état "1" que dans l'état "0" ou vice-versa. Elle est donc passée dans un différentiateur logique DF-2 suivi d'un monostable MS-2 pour lui rendre sa symétrie. L'onde carrée logique est ensuite utilisée pour produire une onde carrée analogique en contrôlant deux commutateurs analogue-digital D/A #2 et D/A #3 aux entrées de l'amplificateur A-2. La sortie de A-2 est alors filtrée par un filtre passe-bande étroit centré à 600 cycles pour se redonner un signal sinusoïdal de phase contrôlée. Le contrôle d'amplitude est fourni par le multiplicateur M-1 dont la deuxième entrée est alimentée par l'intégrateur I-24.

Bloc # 2 Simulation de l'interférence

Pour simplifier, il fut décidé d'utiliser comme signal d'interférence un signal sinusoïdal de 400 cycles de fréquence. Un écart de fréquence aussi important entre ce signal et le signal désiré est nécessaire à cause de la difficulté de simuler des filtres étroits avec assez peu de composantes. Les deux signaux doivent en effet être séparés à l'aide du système de filtrage (bloc # 3).

Le bloc # 2 est essentiellement le même que le bloc # 1 excepté que la portion entre I-10 et C-6 a été ajoutée pour simuler une direction d'arrivée autre que celle du signal. Ce circuit permet d'obtenir, à la sortie de I-15, une onde triangulaire déphasée par rapport à celle qui est donnée par I-10. Cette phase est fixée par la valeur du potentiomètre #34.

Bloc # 3 Système de filtrage

Les sorties des blocs 1 et 2 sont additionnées (A-15) avant d'alimenter le système de filtrage. La circuiterie contenue dans ce bloc a pour but de produire la valeur instantanée de la dérivée de $S/(S+N)$. Ce système contient d'abord deux branches de filtrage; l'une a pour but d'isoler le signal pilote et d'en mesurer la puissance, tandis que l'autre réalise la même opération pour l'interférence. Chaque branche contient res-

pectivement un amplificateur (A-16 et A-17), un filtre passe-bande, un circuit de rectification (M-5 et M-6) et un filtre passe-bas de fréquence de coupure d'environ 10 cycles. La puissance totale (S + N) est obtenue grâce au sommateur (A-20), puis est envoyée à l'une des entrées du diviseur D-1. L'autre entrée du diviseur est alimentée directement à partir de S.

Le diviseur est suivi du dérivateur conçu pour dériver les fréquences en dessous de 3 cycles et pour atténuer les fréquences au-dessus de ce point. Des condensateurs externes ont été utilisés pour sa construction. La sortie du dérivateur est passée dans un circuit limiteur afin de pouvoir amplifier la dérivée tout en évitant la saturation pendant le transitoire au début de chaque période d'opération. Ce signal peut alors être utilisé par le système de contrôle et de commutation pour ajuster les poids jusqu'à la valeur optimale du rapport S/N.

Bloc # 4 Système de contrôle et de commutation

Comme nous l'avons mentionné dans la partie théorique, le taux de changement d'un atténuateur ou d'un déphaseur doit être inversé lorsque la dérivée passe de plus à moins. Le signe de la dérivée est d'abord déterminé par le détecteur de zéro C-9 suivi d'un inverseur logique servant à replacer le signal à la polarité désirée. Ce signal est ensuite fourni à un bistable sensible uniquement au changement du niveau "1" au niveau "0". La sortie du bistable contrôle les entrées de l'amplificateur (A-24) afin d'inverser la polarité du signal à l'entrée de l'intégrateur activé à ce moment.

La commutation d'un intégrateur à l'autre est produite à l'aide d'un ensemble de quatre compteurs $\phi_1$ à $\phi_4$ préalablement ajustés au temps de commutation requis. Un intégrateur est associé à chaque déphaseur ou atténuateur du système. Rappelons toutefois que le nombre de ces derniers doit être doublé afin de pouvoir modifier de la même façon le signal et l'interférence pour chaque antenne. Cette façon d'utiliser les intégrateurs fournit une méthode simple de mémoriser les autres poids pendant que l'un d'eux est ajusté.

## B. RESULTATS DE LA SIMULATION

### a) Expérimentation

La première étape de la simulation sert à vérifier le bon fonctionnement de la boucle d'adaptation. Il est alors préférable d'enlever le plus de complexité possible au système. C'est pourquoi cette vérification a été réalisée pour une boucle qui ne contrôlait qu'un seul déphaseur. La simulation pour un tel système est schématiquement décrite par le diagramme de la Fig. 19. Sur ce diagramme, la sortie des deux premiers sommateurs simule les signaux qui seraient obtenus de deux antennes en présence d'un signal et d'une interférence. Dans ce cas, le signal proviendrait de la direction "broadside" au réseau tandis que l'interférence ferait un angle de 19.5 degrés pour un espacement entre les antennes égal à $\lambda/2$. De plus, on notera que l'amplitude du signal interférent est la même pour les deux antennes, de sorte qu'un déphaseur est suffisant pour l'annuler.

### b) Courbes de fonctionnement

Les formes d'onde en divers points du circuit ont été photographiées pour illustrer que le système fonctionne selon les principes théoriques exposés. La Fig. 20 montre la tension de contrôle du déphaseur (onde triangulaire) en même temps que la valeur de $S/(S+N)$ dans le système. Il apparaît clairement qu'au départ la tension de contrôle est telle que la puissance de N est environ 4 fois plus élevée que S $[10S/(S+N) = 2]$. Le système évolue alors vers la valeur optimale où $10S/(S+N) = 10$. L'intégrateur continue alors à intégrer de sorte que la valeur optimale est excédée. La dérivée de $S/(S+N)$ devient négative, et lorsqu'elle est détectée par le système, le sens d'intégration est inversé, ce qui produit une onde triangulaire. L'amplitude de cette dernière est directement proportionnelle au délai global dans le système, et inversement proportionnelle à la constante de temps de l'intégrateur. On remarquera que les écarts entre la tension de contrôle et la valeur optimale sont perçus sous forme de légères oscillations sur la courbe $S/(S+N)$. L'amplitude de ces oscillations dépend évidemment de l'amplitude de l'onde triangulaire.

La Fig. 21 présente de nouveau la tension de contrôle du déphaseur mais cette fois en corrélation avec la sortie du dérivateur. On peut observer qu'il y a inversion du sens d'intégration à chaque fois que la

dérivée passe de plus à moins. De plus, il est possible d'évaluer à partir de cette figure, le délai global dans le système. Ce délai peut être assimilé au temps que met la dérivée pour redevenir positive après être passée négative et vice-versa. En effet, après l'inversion du signe d'intégration, la dérivée de $S/(S+N)$ au niveau des poids est par définition positive, alors que cela se produit après seulement 100 ms au niveau du dérivateur. C'est le délai total du système que l'on peut considérer comme étant la somme de la constante de temps du dérivateur (50 ms) et du délai de boucle dû en grande partie aux filtres passe-bande (40 ms).

Enfin, la Fig. 22 illustre parfaitement le fonctionnement du contrôle des poids. Sur cette figure, les courbes représentent respectivement de haut en bas, la sortie du détecteur de polarité, la sortie du dérivateur et la sortie du bistable. On remarquera principalement le changement d'état du bistable seulement lorsque la dérivée passe de plus à moins, peu importe l'état où il se trouvait à ce moment. Ce bistable commande directement, on le sait, l'évolution de la tension de contrôle du déphaseur.

c) Comportement et rapidité

Les points importants à considérer pour un système adaptatif sont:

1) la valeur ultime du rapport $S/N$ qui peut être atteinte;
2) la rapidité avec laquelle le système converge;
3) la séparation angulaire minimale entre le signal et une interférence, pour laquelle le système peut fonctionner.

En ce qui concerne le système que nous considérons, ces caractéristiques ne sont pas indépendantes.

La séparation angulaire dépend à la fois du bruit interne généré par la boucle, et de l'amplitude de la dérivée elle-même. L'amplitude de la dérivée doit surpasser le niveau de bruit interne pour être détectable. Plus le signal et l'interférence sont rapprochés l'un de l'autre angulairement, plus la dérivée diminue puisque la puissance de l'un et l'autre tend à varier de la même façon. D'autre part, on a

$$\frac{d}{dt}\frac{S}{(S+N)} = \frac{d}{d\phi}\frac{S}{(S+N)} \cdot \frac{d\phi}{dt} \quad .$$

On peut donc augmenter la valeur de la dérivée en variant plus rapidement

la tension de contrôle du déphaseur. Il en résultera cependant des oscillations plus fortes sur le rapport S/N du système. Cependant, une augmentation de la constante de temps du dérivateur réduirait le bruit dans le système et améliorerait le point 3). La rapidité de convergence serait alors réduite.

La valeur ultime du rapport S/N pour un système non linéaire est plus difficile à définir. Le rapport S/N oscille, en effet, entre la valeur fixée par le bruit interne du système et une valeur qui dépend du taux de changement de la tension de contrôle. En d'autres termes, la valeur de S/N varie dans le temps et l'amplitude de cette variation peut être réduite ou changée à volonté. Pour un système donné, la rapidité de convergence sera d'autant plus faible que les oscillations sur S/N sont faibles.

Un autre facteur important dans la performande du système est le délai total de boucle. Ce dernier fixe le temps nécessaire pour que le système produise une inversion de commande. Le délai de boucle est donc la limite fondamentale à la rapidité de convergence. Pour une variation de S/N donnée, le système pourra être d'autant plus rapide que le délai de boucle est faible.

En résumé, les facteurs qui limitent ou fixent la rapidité de convergence sont:

- le délai total de boucle,
- l'amplitude qu'il faut se donner sur la variation du rapport S/N,
- la séparation angulaire minimale entre S et N.

d) Rapidité de la boucle de simulation

Etant donné que l'amplitude des oscillations sur le rapport S/N dépend à la fois de S et de N, et aussi du nombre de poids dans le système, nous parlerons plutôt de la rapidité en relation avec l'écart entre la tension de contrôle et la valeur optimale. Pour la boucle simulée, les courbes montrent, pour un écart de .45 V de la valeur optimale, un temps de réponse maximal de 4 s ou un temps moyen de 1.15 s. Notons que .45 V dans ce système correspond à un écart de phase de 9°. Le temps moyen de convergence pour un écart de phase de 1° aurait été 9 fois plus grand, c'est-à-dire 10.5 secondes. Le temps de réponse de boucle est aussi di-

rectement proportionnel au délai total de boucle qui est de 100 ms. Un délai de boucle de 1 ms aurait par conséquent produit un temps de réponse moyen de 105 ms. Pour le système réel en laboratoire, on pense pouvoir obtenir un délai de boucle de l'ordre de 10 μs, ce qui serait 10,000 fois plus rapide que le système de simulation.

## Annexe II

# AN ADAPTIVE ARRAY WITH "ON-OFF" AUTOMATIC CONTROL

J.A. Cummins, G.Y. Delisle and M.G. Pelletier

# AN ADAPTIVE ARRAY WITH "ON-OFF" AUTOMATIC CONTROL

J.A. Cummins, G.Y. Delisle and M.G. Pelletier

Department of Electrical Engineering, Laval University, Quebec, Canada G1K 7P4

## INTRODUCTION

Since the publication in 1967 of the now classic paper by Widrow and his co-workers, on adaptive array antenna systems (1), the various methods that were proposed for processing antenna signals adaptively have aroused an ever increasing interest (2,3). In applications involving telecommunications, a variety of methods may be used for controlling the array weights. The best known are the gradient technique implemented with a least-mean-square (LMS) algorithm (4) and the sample matrix inversion technique (5). The technique that we propose is a form of the gradient technique implemented through the repeated use of a servomechanism loop of the "on-off" type.

## ADAPTIVE PROCESSING OF ANTENNA SIGNALS

Figure 1 illustrates the adaptive method of antenna processing that we are considering. It is apparent, at once, that this method is radically different from those that are currently proposed for radar application in which a signal derived from a priori known information is injected into the system. Use is made, instead, of a pilot signal, or "beacon", which is assumed present, either within or slightly outside the signal frequency spectrum. Postulating the presence of such a pilot signal is not a severe limitation, since it is often part of the desired signal, or at least could be easily incorporated to it. Because of the sequential adjustments of the weights, this system should give best results with high gain antennas or with multibeam antennas. Indeed, in sequential systems, the settling time grows more rapidly with the number of elements than in conventional systems, in spite of the fact that nonlinear adaptive loops are faster than linear loops.

The system operates as follows: the antenna signals are "weighted" in amplitude and phase, summed and lowered in frequency with a local oscillator and a mixer. The mixer output is divided into two parts, one of which is demodulated to gather the transmitted information while the other is used to perform the adaptive control.

In the control loop, appropriate band pass filters isolate the pilot signal in one branch and route via another branch a wider portion of the spectrum containing the useful signal, the noise, the interference if present and possibly the pilot signal also. The output from both branches are rectified yielding DC voltages proportional to the respective power of each branch. The voltage proportional to the interfering power is then subtracted from the other voltage which is representative of the amount of pilot signal power. If we postulate that signal and interference are not originating from the same direction, the difference will be maximized after the antenna weights are adjusted in such a way that a null is presented in the direction of the interference. The time derivative of the power difference between the two branches is used as a control signal for adjusting the antenna weights.

This method of adaptive antenna signal processing has several distinctive characteristics:

a) a portion of the transmitted signal is used for identifying its direction of arrival;
b) the weighting given to the output of each element in the array is implemented by means of electronically controlled phase shifters and by electronically controlled attenuators. The latter could be replaced by variable gain amplifiers;
c) the weights are adjusted sequentially;
d) the servo-loops are of the type designated as "on-off" in servomechanism literature;
e) the system can be used either with multi-beam antennas or with arrays of highly directive antennas.

## THEORETICAL CONSIDERATIONS

The parameter to be optimized is the S/N ratio which bears a direct relation to the weights. However, the servo-loop uses the time derivative of S/N to perform the optimization. This can be understood by considering the properties of the adaptive algorithm.

### Adaptive Algorithm

Let $W_i = w_i e^{j\phi_i}$ be the complex weight associated with the $i^{th}$ antenna element, where $w_i$ is the amplitude and $\phi_i$ the phase of $W_i$.

The variation $\Delta(S/N)$ of the S/N ratio depends on the weights; for the $i^{th}$ weight, its expression is:

$$\Delta(S/N) = \frac{\partial(S/N)}{\partial w_i}\Delta w_i + \frac{\partial(S/N)}{\partial \phi_i}\Delta\phi_i \qquad (1)$$

We may consider the S/N, at the output of the summer, as a functional of a vector V consisting of the 2n components of the weights, that is:

$$V = (\omega_1, \omega_2, \ldots, \omega_n, \phi_1, \phi_2, \ldots, \phi_n).$$

It has been shown (6) that the fastest increase in S/N is in the direction defined by the following gradient:

$$\nabla(S/N) = \left(\frac{\partial(S/N)}{\partial w_1}\ldots\frac{\partial(S/N)}{\partial w_n}, \frac{\partial(S/N)}{\partial \phi_1}\ldots\frac{\partial(S/N)}{\partial \phi_n}\right) \qquad (2)$$

Equation (2) implies that the increase in S/N can be made gradually.

If the increase in (S/N) is achieved one step at a time, then the weights at step (n+1) are related to those at the previous step n by equations (3) and (4) below:

$$w_i^{(n+1)} = w_i^{(n)} + \alpha \frac{\partial(S/N)}{\partial w_i} \qquad (3)$$

and

$$\phi_i^{(n+1)} = \phi_i^{(n)} + \beta \frac{\partial(S/N)}{\partial \phi_i} \qquad (4)$$

where $\alpha$ and $\beta$ are small positive real constants. The parameters $\alpha$ and $\beta$ must be sufficiently small for stability, but strong enough for reasonably rapid convergence.

In equation (2), the derivation of (S/N) is taken with respect to $w_i$ or $\phi_i$, but the time derivative of S/N can also be used as a criterion for determining how the weights are to be changed at each step.

Assuming that a small change takes place in $w_i$, the first order change in (S/N) is:

$$\Delta(S/N) = \frac{\partial(S/N)}{\partial w_i} \Delta w_i \qquad (5)$$

which is equal to:

$$\Delta(S/N) = \frac{\partial(S/N)}{\partial t} \cdot \frac{\partial t}{\partial w_i} \nabla w_i \qquad (6)$$

or equivalently,

$$\Delta(S/N) = \frac{\partial(S/N)}{\partial t} \cdot \frac{\Delta w_i}{\frac{\partial w_i}{\partial t}} \qquad (7)$$

Because the quantity $\Delta w_i/(\partial w_i/\partial t)$ is always positive, equation (7) may be rewritten:

$$\Delta(S/N) = \frac{\partial(S/N)}{\partial t} \cdot k|\Delta w_i| \qquad (8)$$

where k is a positive constant.

Equation (8) implies that $\partial(S/N)/\partial t$ must be positive for the S/N ratio to increase. Therefore our task is to find the sign of $\Delta w_i$ which will make $\partial(S/N)/\partial t$ positive.

The above reasoning is quite similar to the logic underlying the operation of the "on-off" type of servomechanisms. Expressed in simple terms, this logic is equivalent to the following statement: "If a change in the control improves the desired output, the sign for the next change must be kept the same as it was in the previous one, otherwise it must be reversed".

## Control Law in the "On-off" Type of Servomechanism

Figure 2a shows the schematic diagram of a single loop servomechanism with time derivative control (7). In this class of servomechanisms, the control system uses the error dy/dt to perform a dx/dt command on the process. For the "on-off" type, the control law is generally such that it can be expressed by the following equation:

$$\frac{dx}{dt} = \kappa \operatorname{sign} \frac{dy/dt}{dx/dt} = \kappa \operatorname{sign} \varepsilon \qquad (9)$$

where $\kappa$ is a positive constant and sign $\varepsilon$ means the sign of (dy/dt)/(dx/dt).

It is apparent from (9) that the absolute value of the command signal dx/dt does not depend on the error signal dy/dt. In the search for a maximum value of y (which corresponds to S/N in our case) equation (9) may be interpreted to mean the following: "As long as dy/dt is positive, the sign of the control signal must remain unchanged; if dy/dt becomes negative, the sign of the control signal must be reversed except when dy/dt changes from a negative to a positive value.

Typical Response of "On-off" Servomechanisms. The typical response of an "on-off" servomechanism is illustrated in Figure 3a (8). It can be seen that permanent oscillations are present. These oscillations are inherent to the limited time response of the system. An increase of the oscillation frequency will in general reduce the amplitude of the oscillations (Figure 3b).

## Dynamics of the Process

In addition to the delay due to commutation, limited time response also occurs in

a) the detection of the error signal (the change in S/N is not instantaneously detected;
b) the process itself (the response to the control signal is not instantaneous).

This is schematically illustrated by the addition of transfer functions boxes in the loop as shown in figure 2b.

Dynamics of the Error Signal Detection. The system will converge to the optimum solution unless drifts are present in the characteristics of the process (7). These drifts can be interpreted as changes in the position of the signal source or of the interference.

Dynamics of the Process Itself. In figure 2b, if a linear first order relationship is assumed between v and x, the ratio F(p) of the Laplace transforms X(p) and V(p) of x and v, respectively may be written:

$$F(p) = \frac{X(p)}{V(p)} = \frac{1}{1 + \tau p} \qquad (10)$$

It can be shown that the system is stable if

$$|x - v| < |\kappa\tau| \quad \text{at} \quad t = 0$$

where $\kappa = \pm |dx/dt|$ .

For a ramp signal v (which is our case), $|x - v|$ is never greater than $|\kappa\tau|$ and the system is stable.

## EXPERIMENTAL PROGRAM

The experimental realization of a laboratory prototype of a single adaptive loop will constitute a most decisive factor in evaluating the practicality of the system. A single loop controlling a phase shifter is presently under experimentation. Figure 4 shows the schematic diagram of this simple realization. In this experiment, signal and noise are sine waves of different frequencies simulated by a divider-combiner arrangement.

The processing used for the detection of d(S/N)/dt may be implemented in various ways. In the selection of a processing method both the merits of the processing itself and the availability and the limitations of the electronic components that must be used to implement it, must be considered. The criterion to be optimized is the S/N whose time derivative is:

$$\frac{d(S/N)}{dt} = \frac{N(dS/dt) - S(dN/dt)}{N^2} \qquad (11)$$

If this expression were to be implemented as it stands, the sensitivity would vary greatly with N, being quite sensitive for N small, but very insensitive for N large. Fortunately in "on-off" servomechanisms only the sign of d(S/N)/dt is really important. A processing method that really performs the operation N(dS/dt) - S(dN/dt) and thus obviates the disadvantage mentioned above is experimented. Another processing method based upon the derivative of S/S+N is also under experimental evaluation.

## CONCLUSION

A method was presented of discriminating against interference by using an adaptive algorithm operating in real time on the received signals of the array. The system operates by adjusting sequentially in amplitude and phase, the weights given to each element of the array. The closed loop circuits that control the adjustments of the weights are of the type designated as "on-off" in servo-mechanism literature.

Acknowledgement. The research for this project has been supported by Communications Research Centre, Ottawa, Canada, under contract OSU77-00305.

## REFERENCES


1. Widrow, B. et al, 1967, "Adaptive antenna systems", Proc. IEEE, 55, 2143-2159.
2. Special Issue on Adaptive Antennas, 1976, IEEE Trans. Antennas Propagat., AP-24.
3. Gabriel, W.F., 1976, "Adaptive arrays - an introduction", Proc. IEEE, 64, 239-272.
4. Widrow, B., 1966, "Adaptive filters I: Fundamentals", Stanford Univ. Electronics Labs., Tech. Rep. 6764-6.
5. Reed, I.S. et al, 1974, "Sample matrix inversion technique", Proc. Adaptive Ant. System Workshop, NRL, Washington, D.C., 219.
6. Shor, S.W.W., 1966, "Adaptive technique to discriminate against coherent noise in a narrow-band system", J. Acoust. Soc. Amer., 39, 74-78.
7. Decaulne, P., Gille, J.-Ch., et Pelegrin, M., 1976, "Introduction aux systèmes asservis extrémaux et adaptatifs", Dunod, Paris.
8. Gille, J.-Ch., Decaulne, P., et Pelegrin, M., 1976, "Systèmes asservis non linéaires", Tome 1, Dunod, Paris.


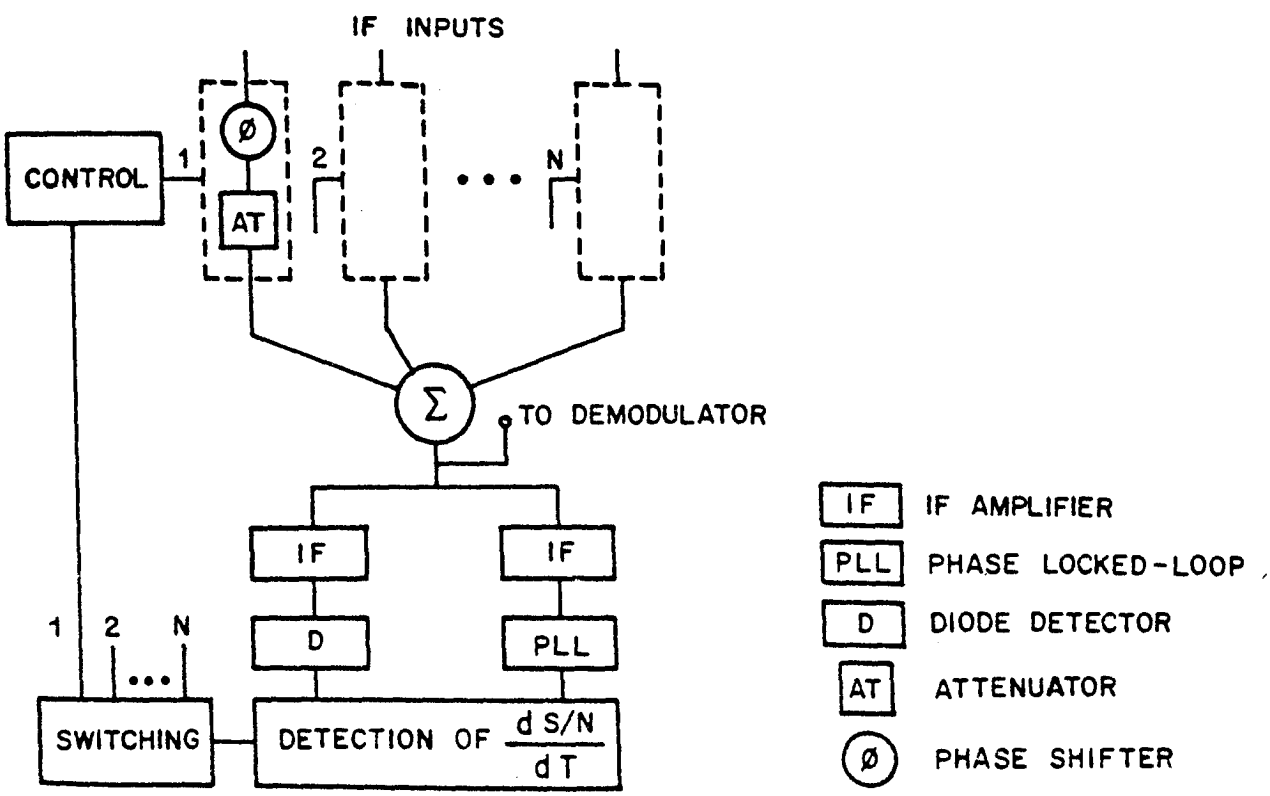


Figure 1 Schematic diagram of the adaptive system.

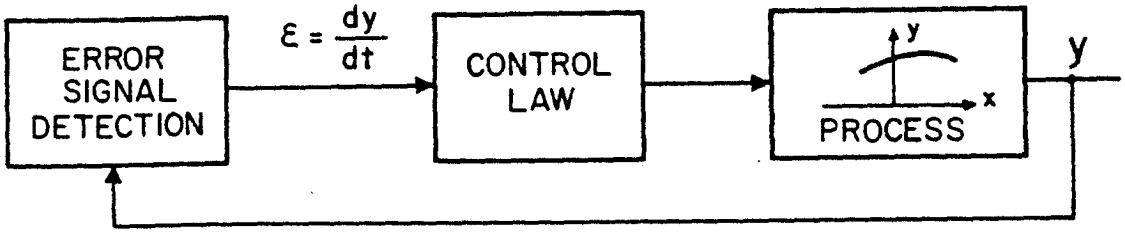


a)

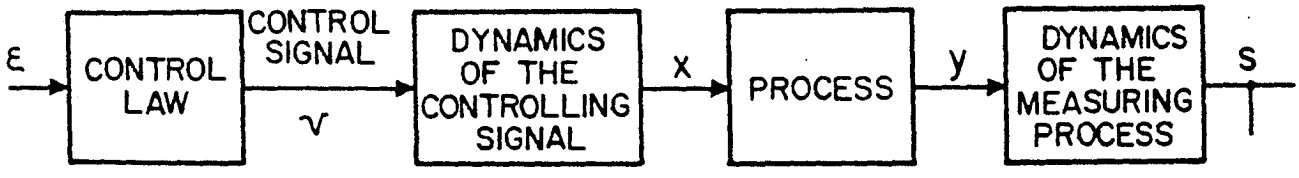


b)

Figure 2-a) Servomechanism diagram with time derivative control.

Figure 2-b) Diagram including dynamical effects.

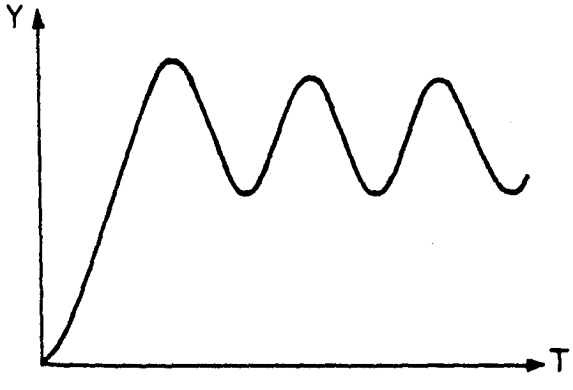


a)

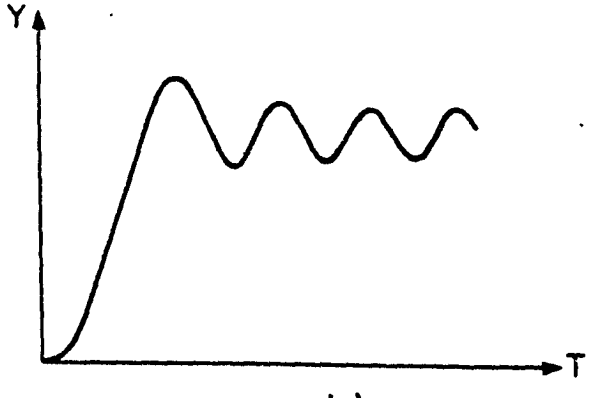


b)

Figure 3-a) Typical response of an "on-off" servomechanism.

Figure 3-b) Smaller amplitude oscillations response.

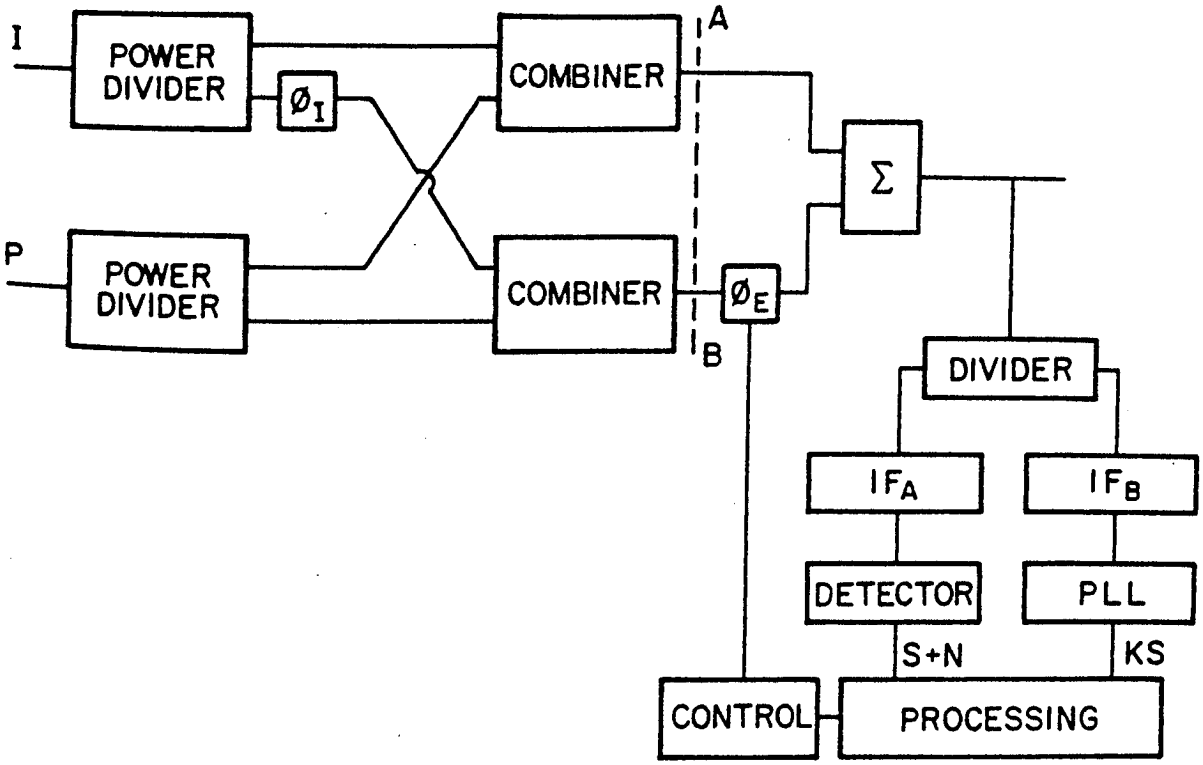


Figure 4 Set-up used for the experimentation of an adaptive loop.

# F I G U R E S

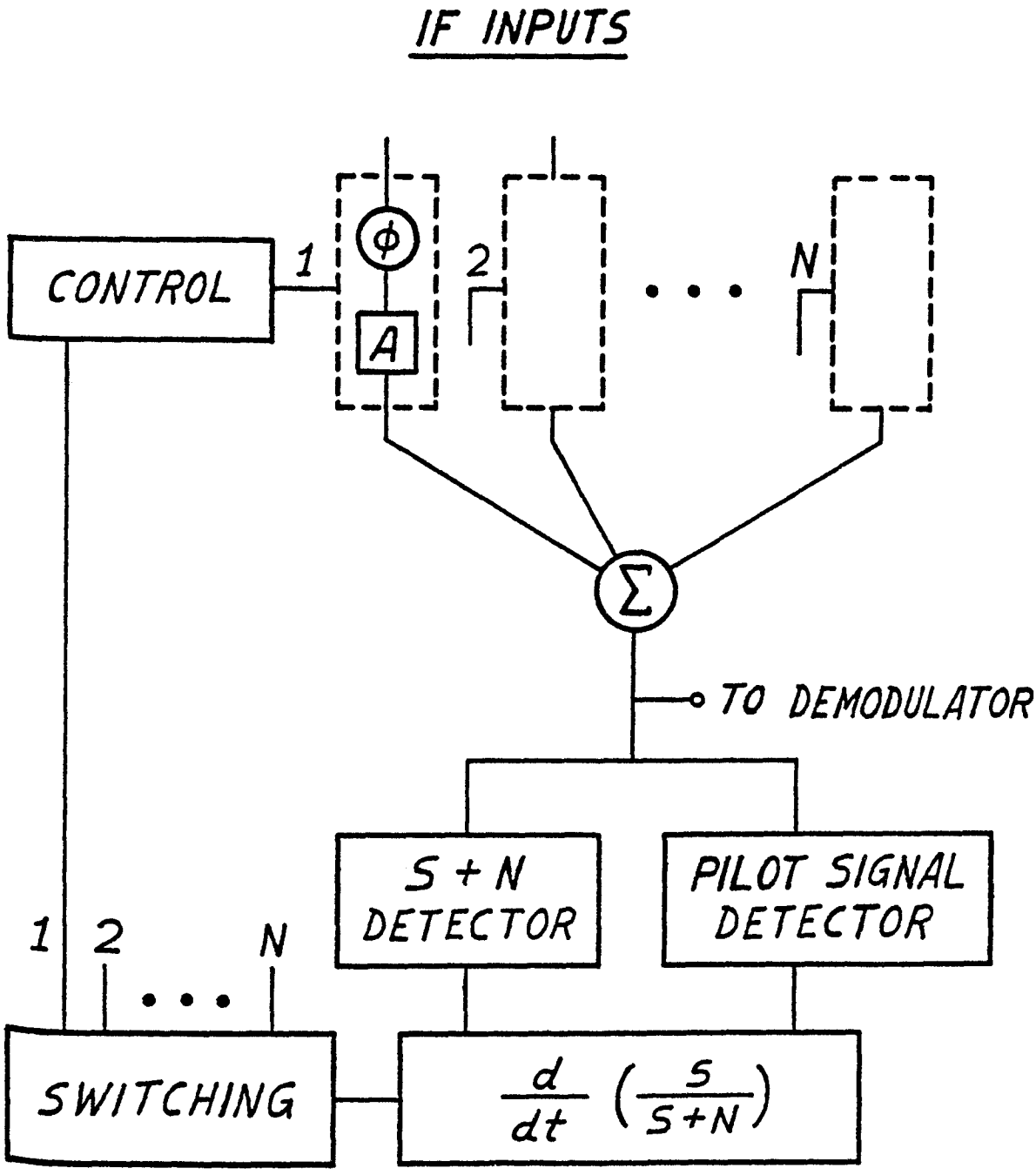


Fig. 1: Schematic diagram of the adaptive system.

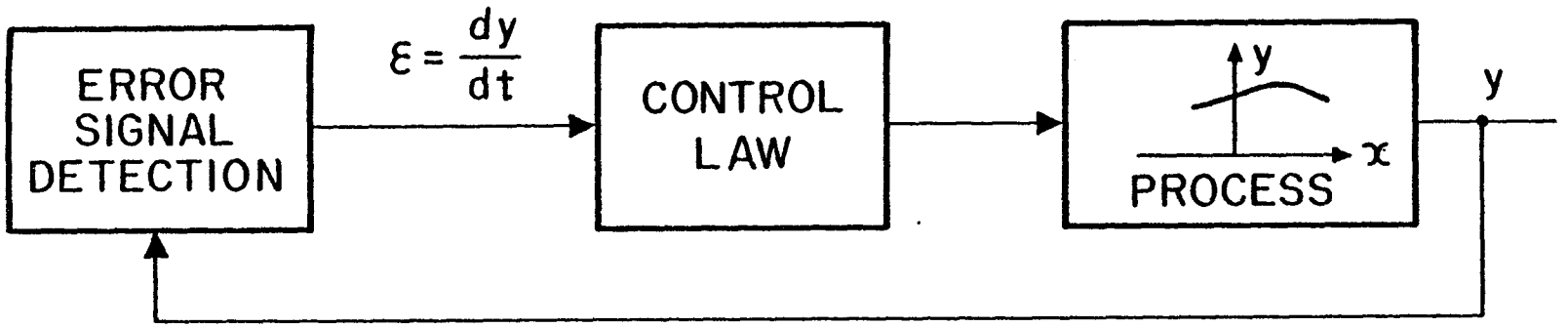


(a)

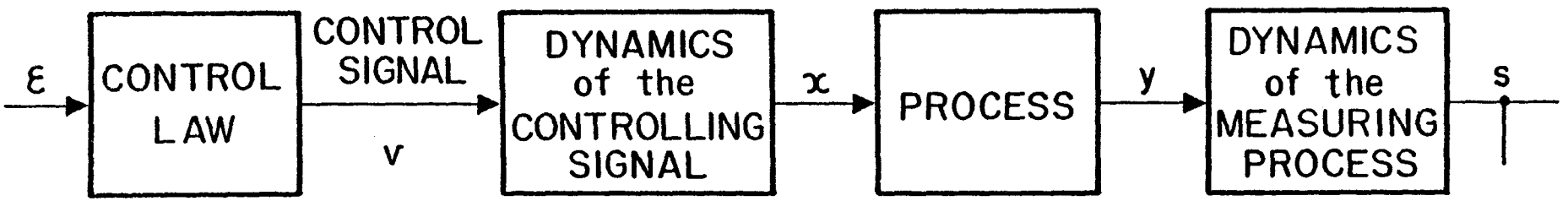


(b)

Fig. 2: a) Servomechanism diagram with time derivative control;
b) Diagram including dynamical effects.

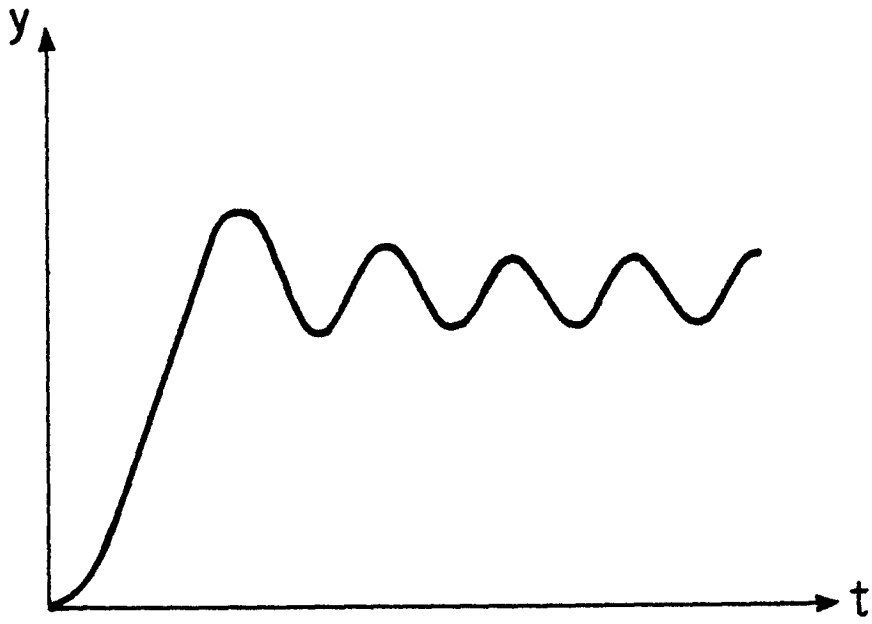


(a)

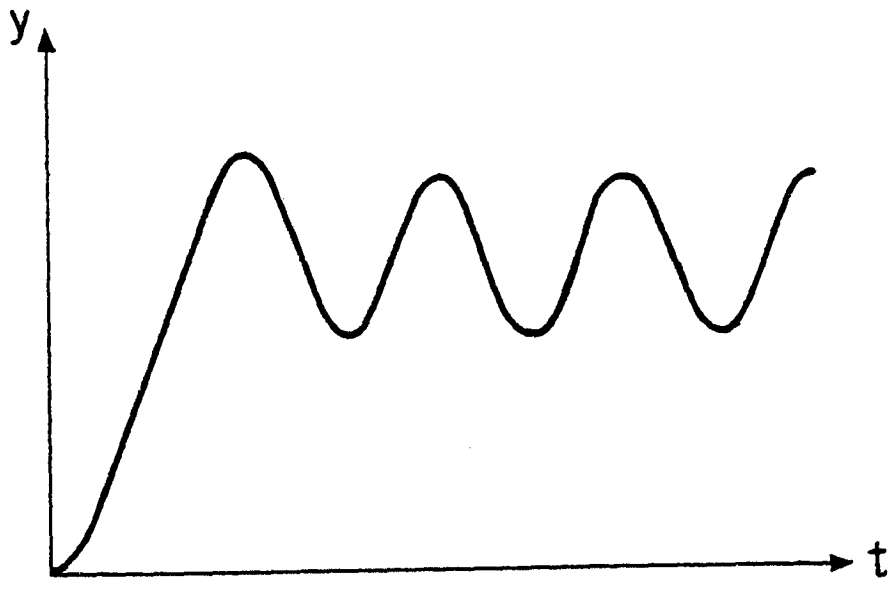


(b)

Fig. 3: Typical responses of an "on-off" servomechanism.

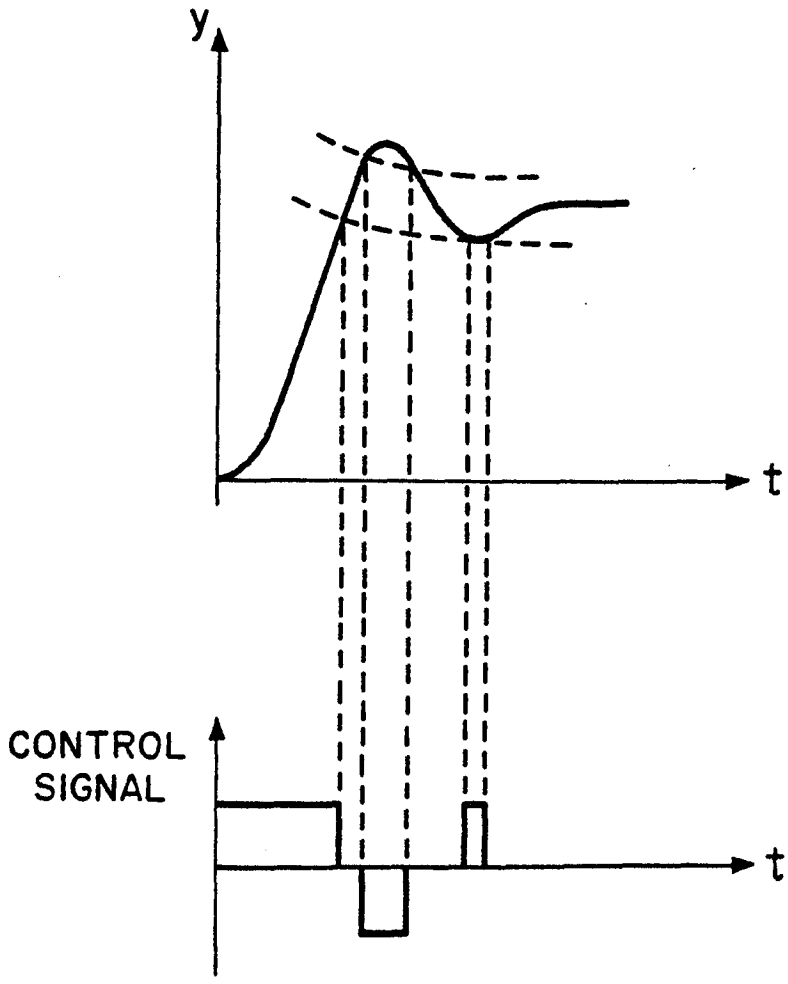


Fig. 4: The effect of idle times on the response of "on-off" servomechanisms.

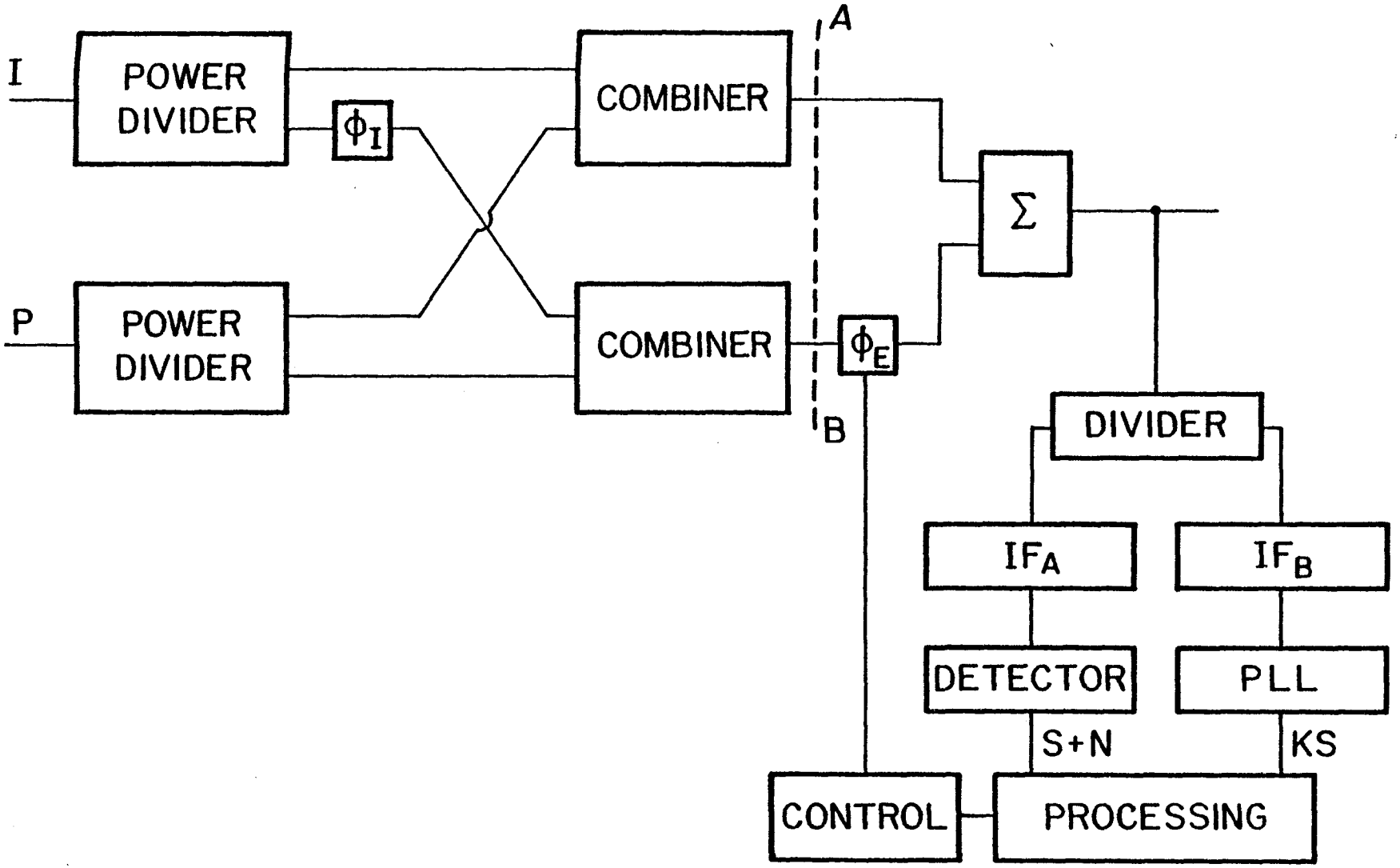


Fig. 5: Set-up used for the experimentation of an adaptive loop.

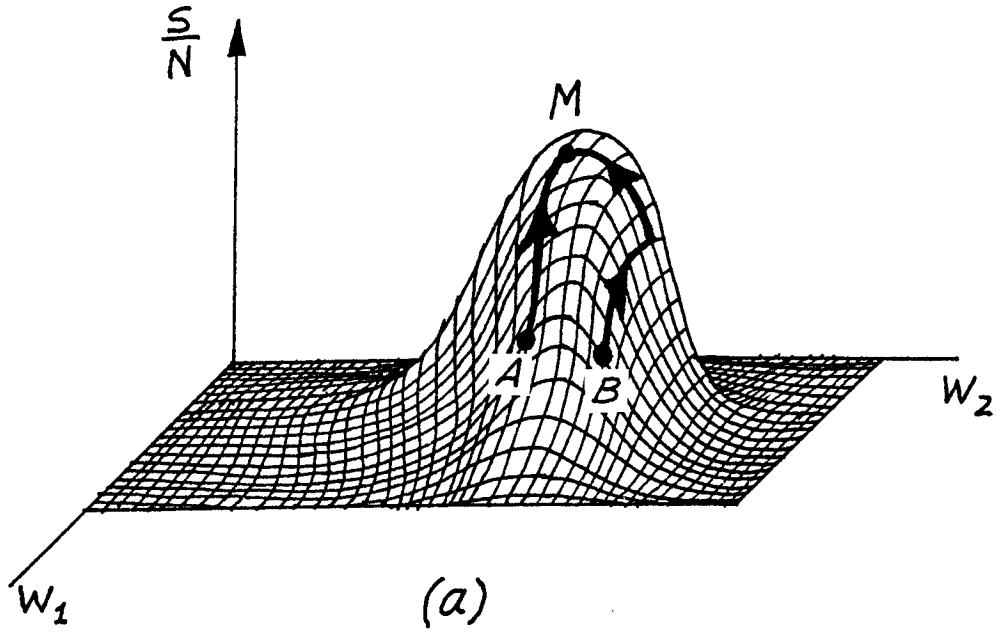


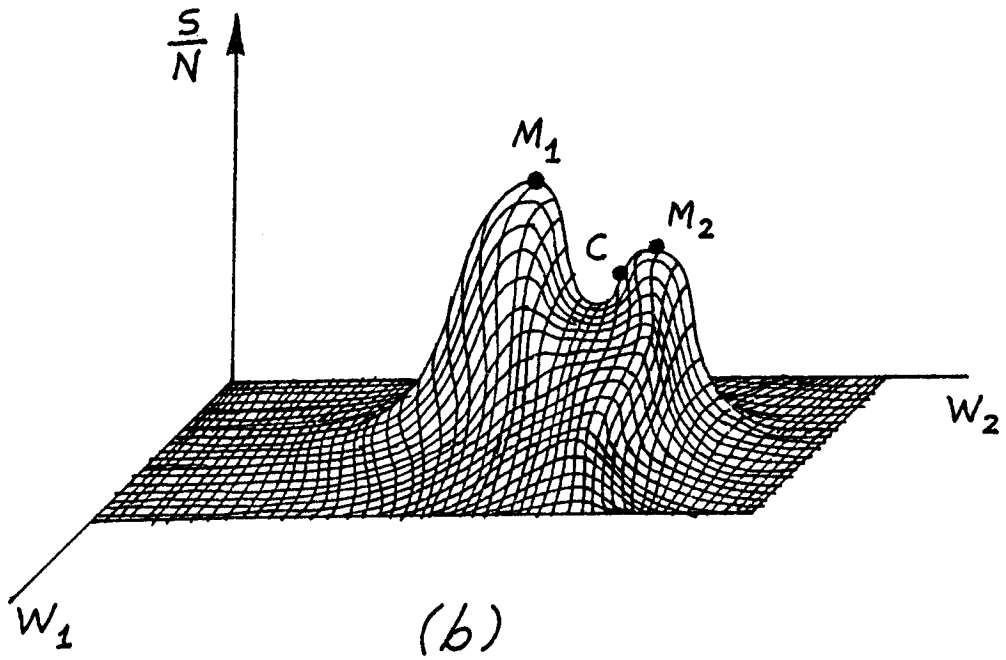


Fig. 6: Two-dimensional representations of the signal-to-noise ratio: a) with a single maximum, b) with two maximums.

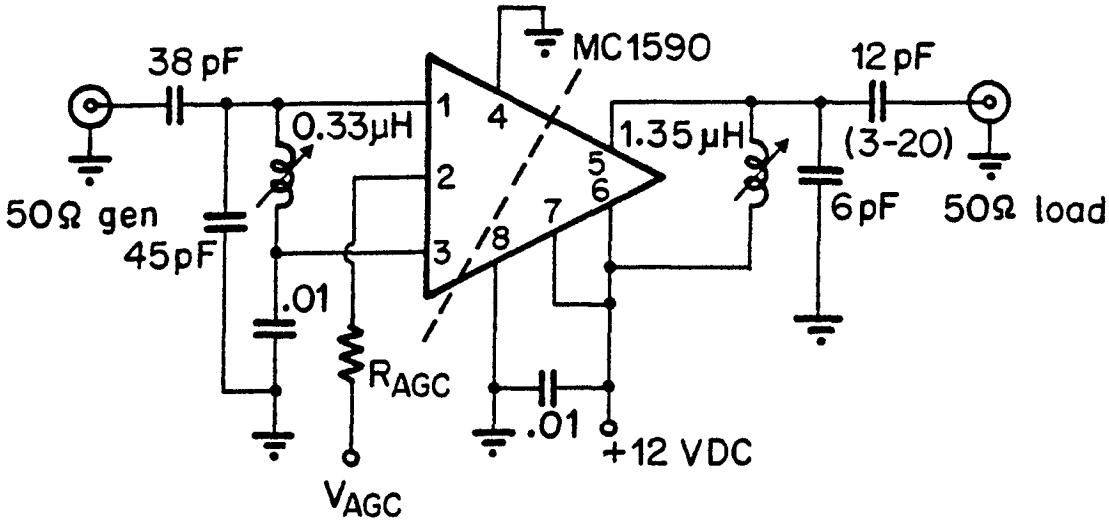


(a)

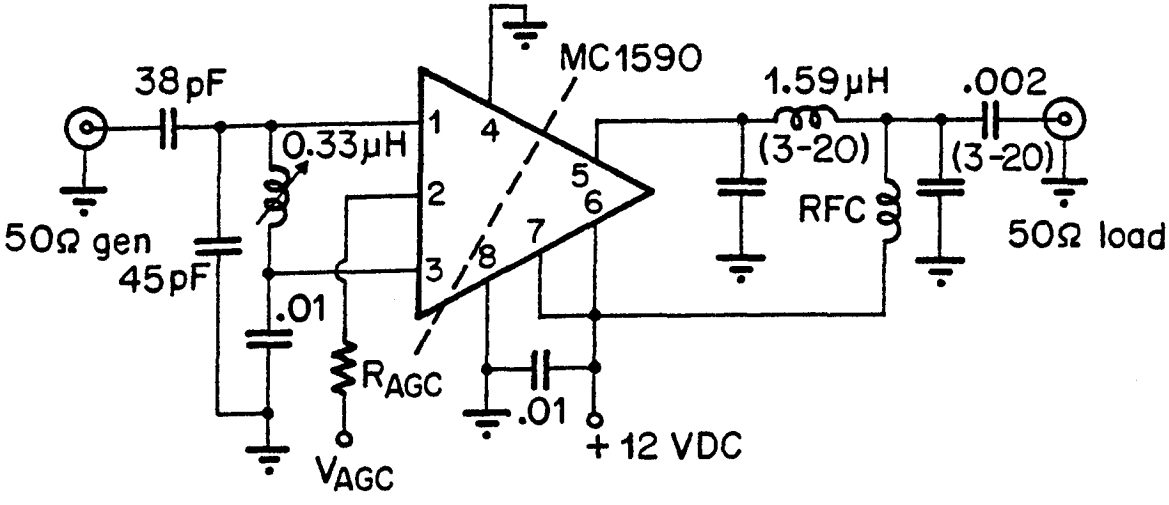


(b)

Fig. 7: IF amplifiers: a) in the phased-locked-loop branch, b) in the power sensor branch.

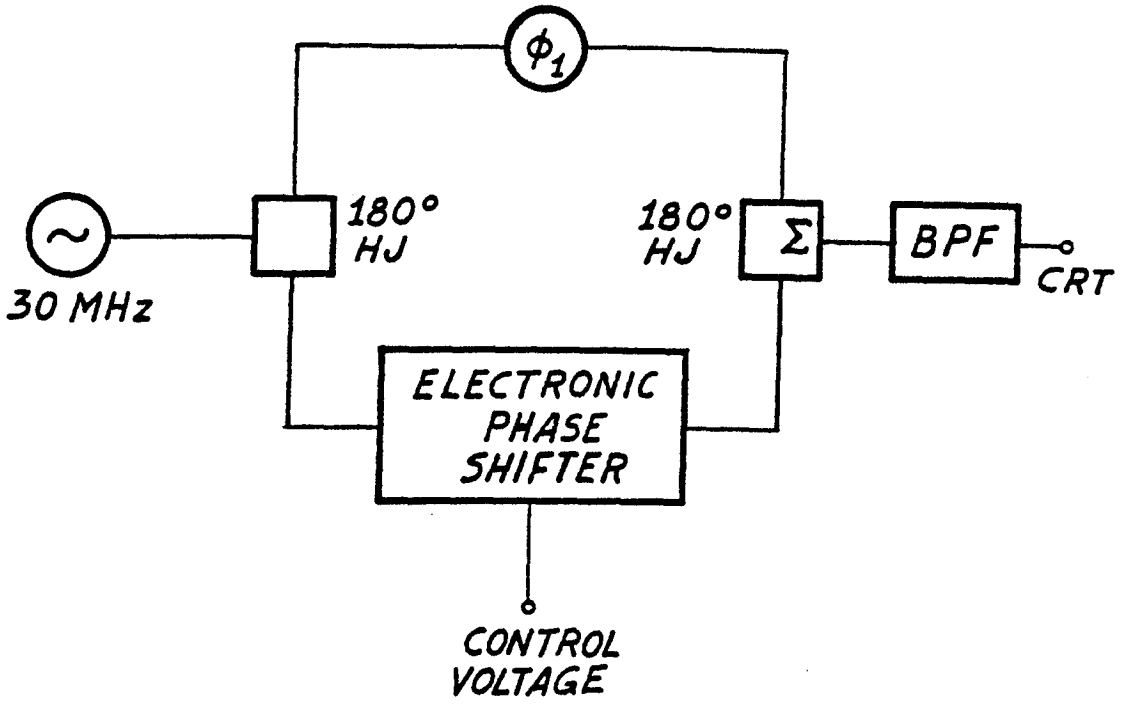


(a)

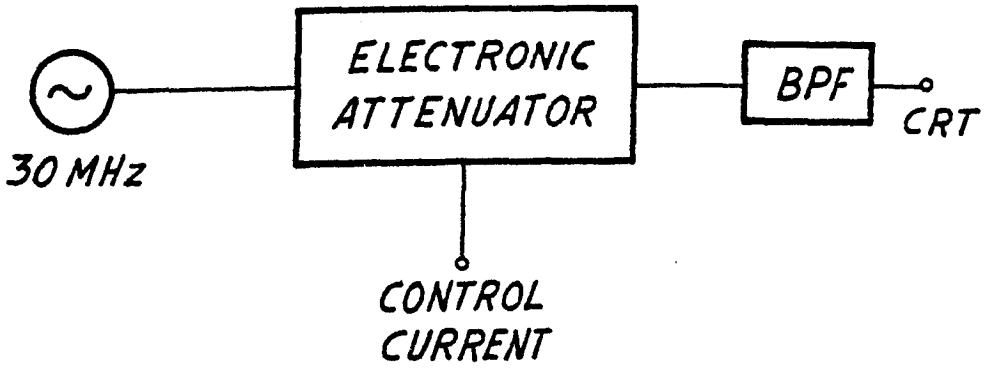


(b)

Fig. 8: Set-up used for the time response measurement of a) the electronic phase shifters, b) the electronic attenuators.

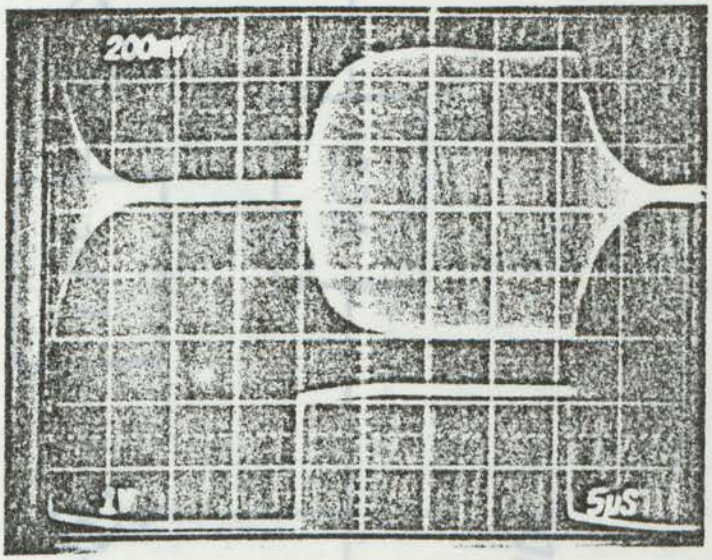


Fig. 9: The electronic phase shifters time response.

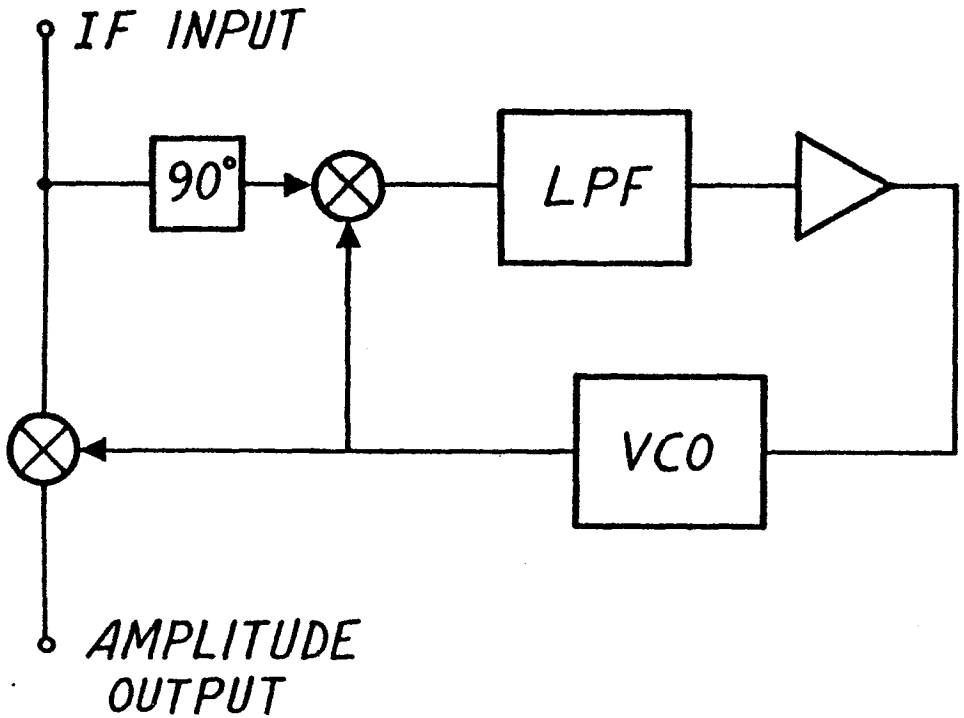


Fig. 10: Pilot signal detector.

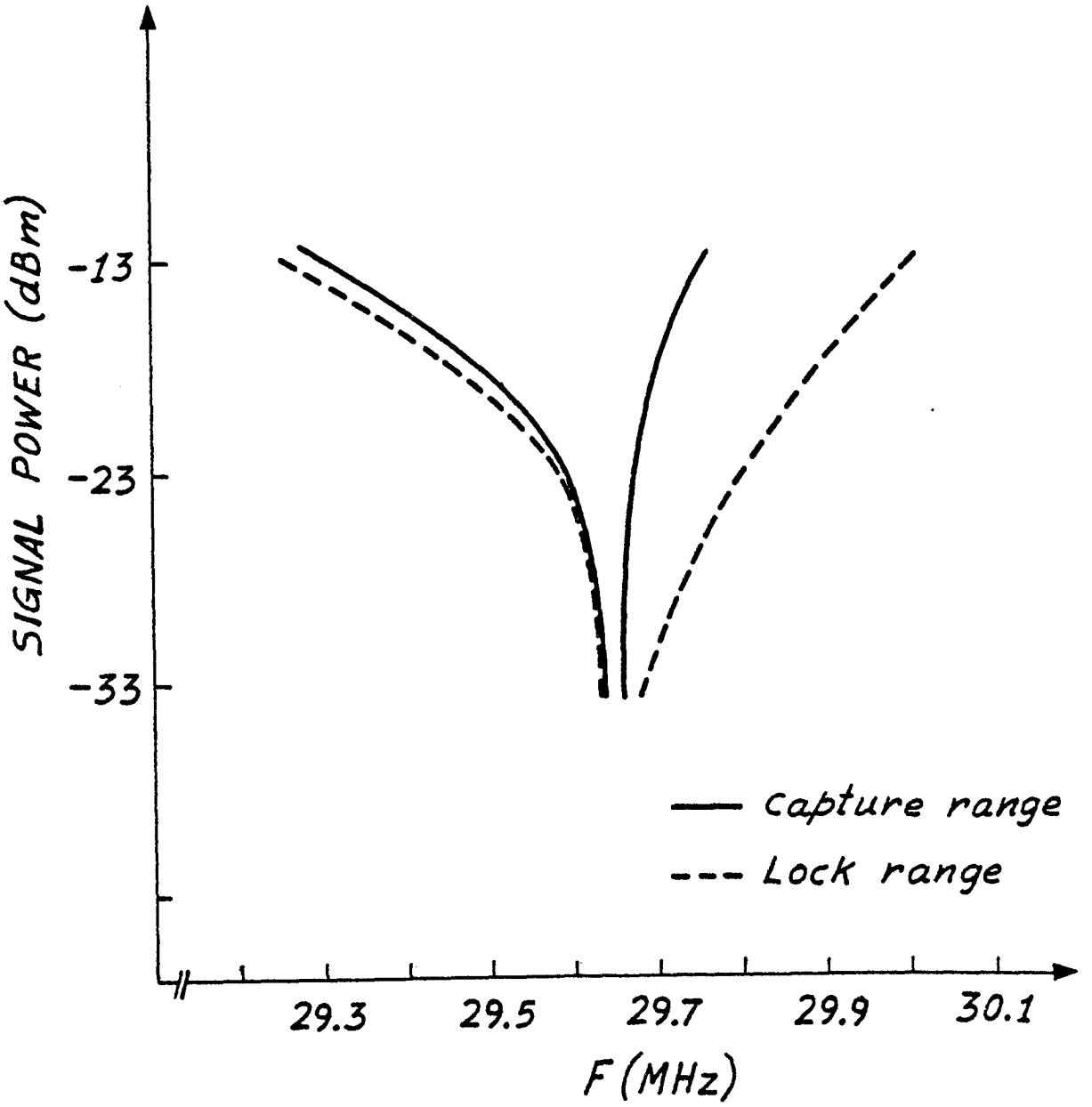


Fig. 11: The capture and the lock range of the phased-locked-loop as function of the applied signal power.

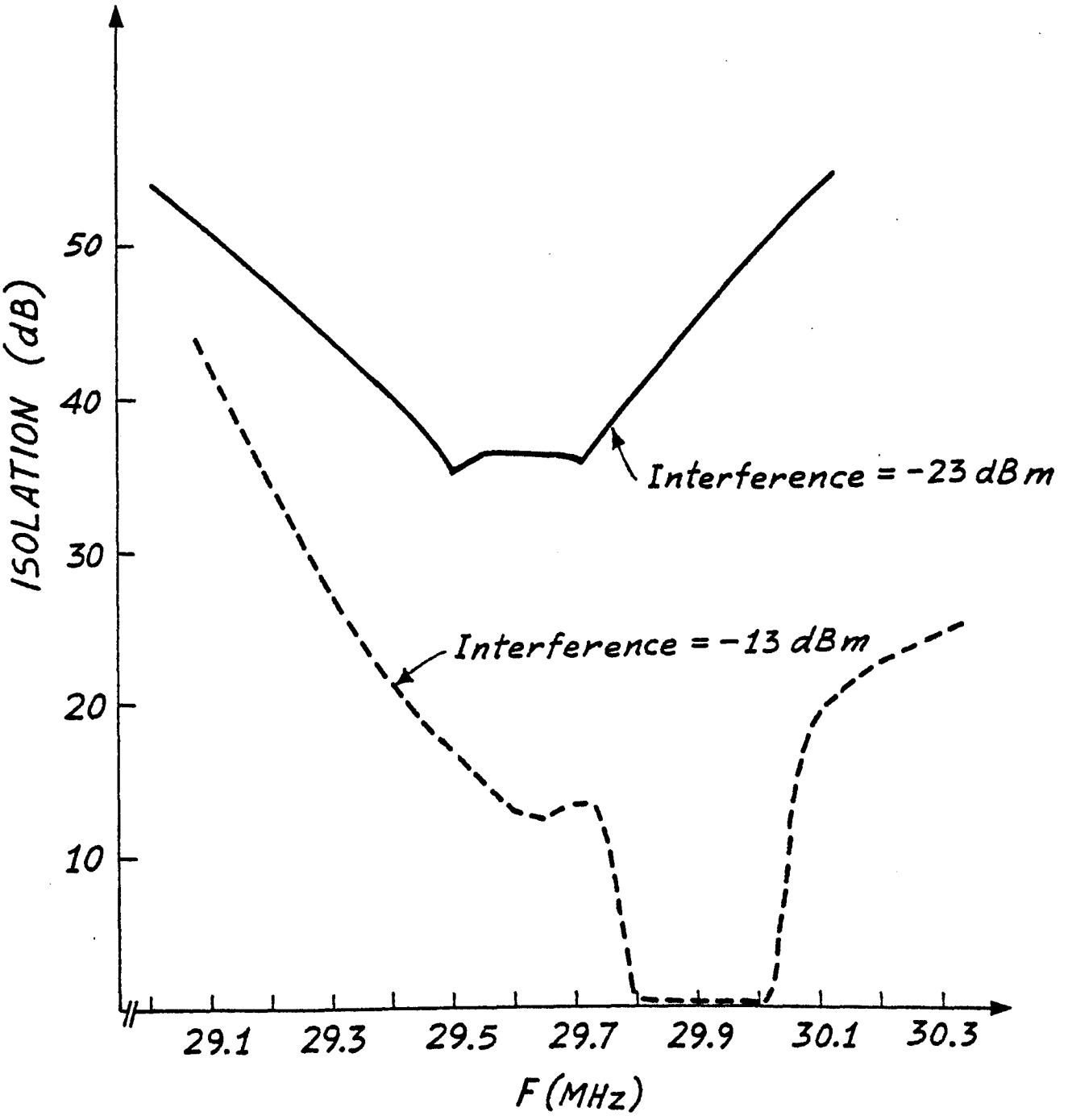


Fig. 12: Interference to pilot isolation (pilot = -13 dBm)

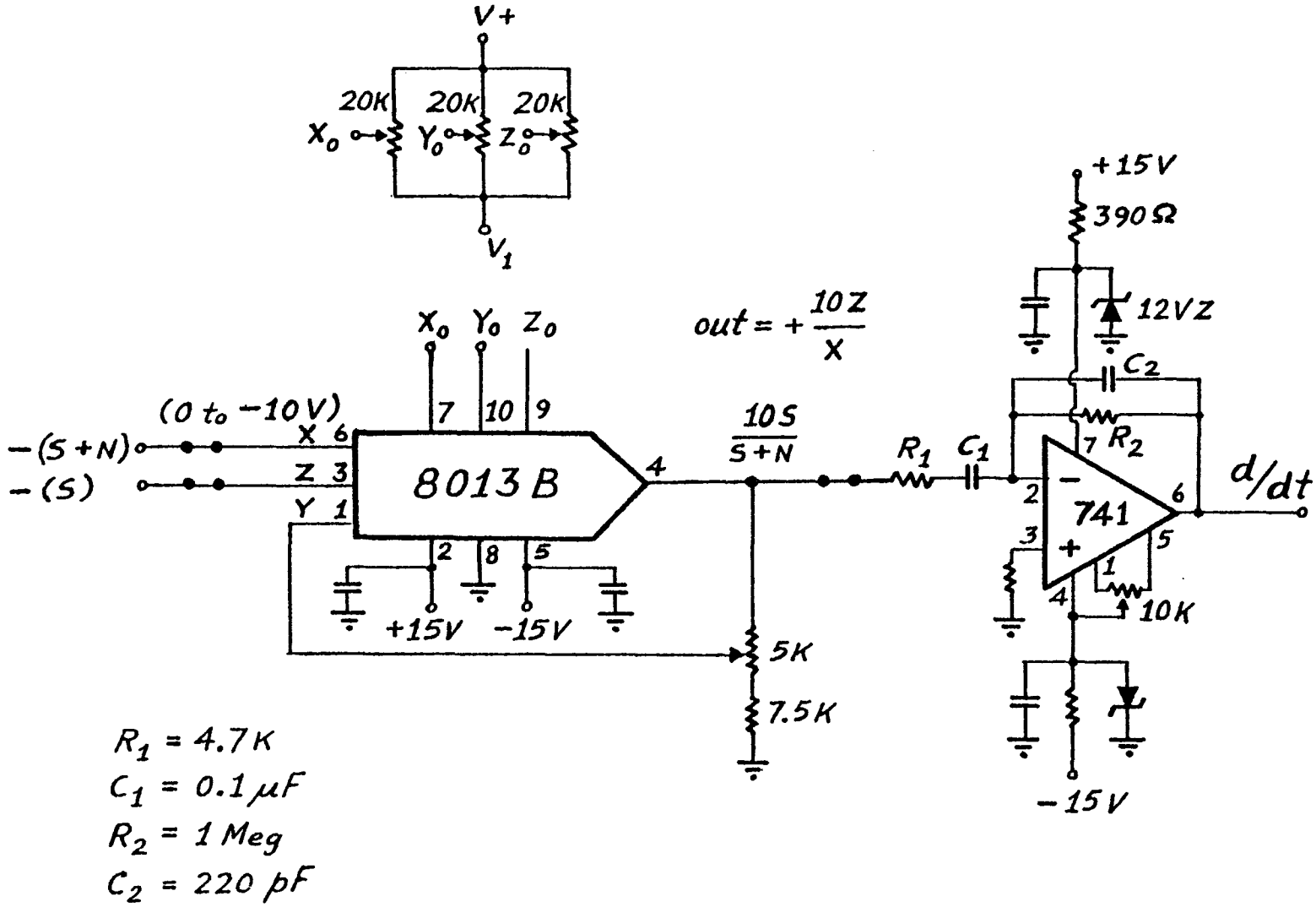


Fig. 13: Implementation of $10\,\frac{d\left(\frac{S}{S+N}\right)}{dt}$ as the error signal.

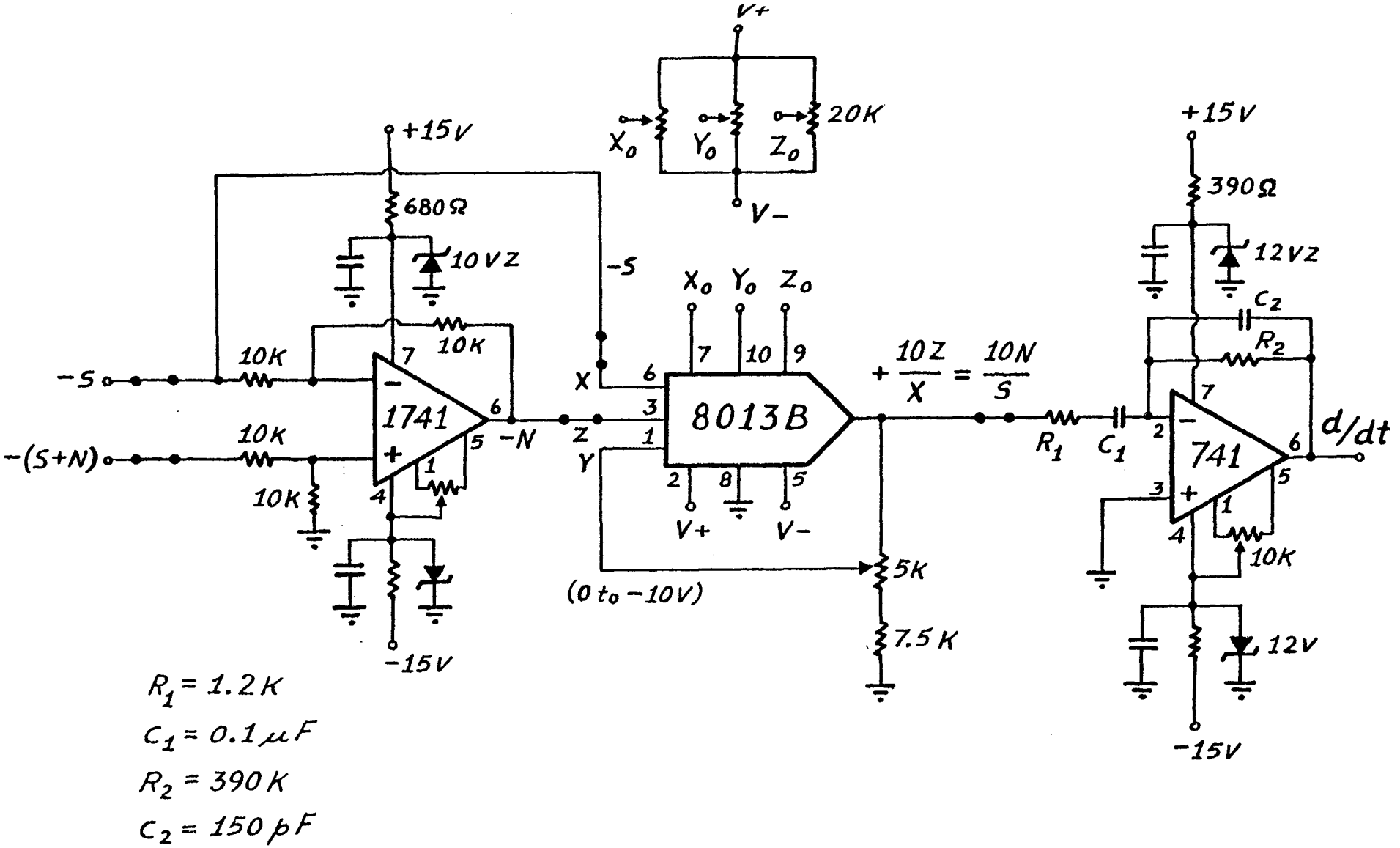


Fig. 14: Implementation of $10\,\dfrac{d\left(\frac{N}{S}\right)}{dt}$ as the error signal.

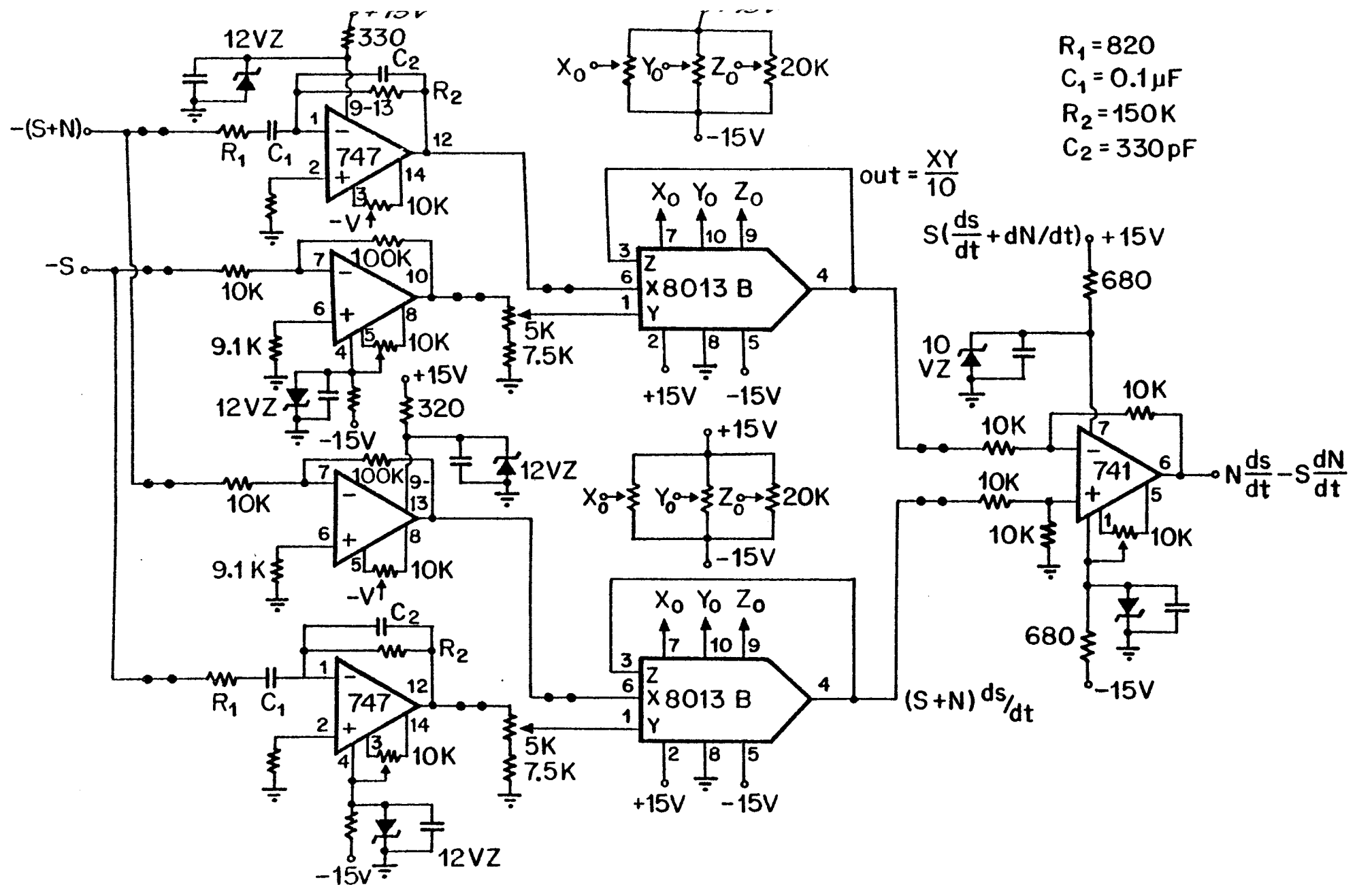


Fig. 15: Implementation of N(dS/dt) - S(dN/dt) as the error signal.

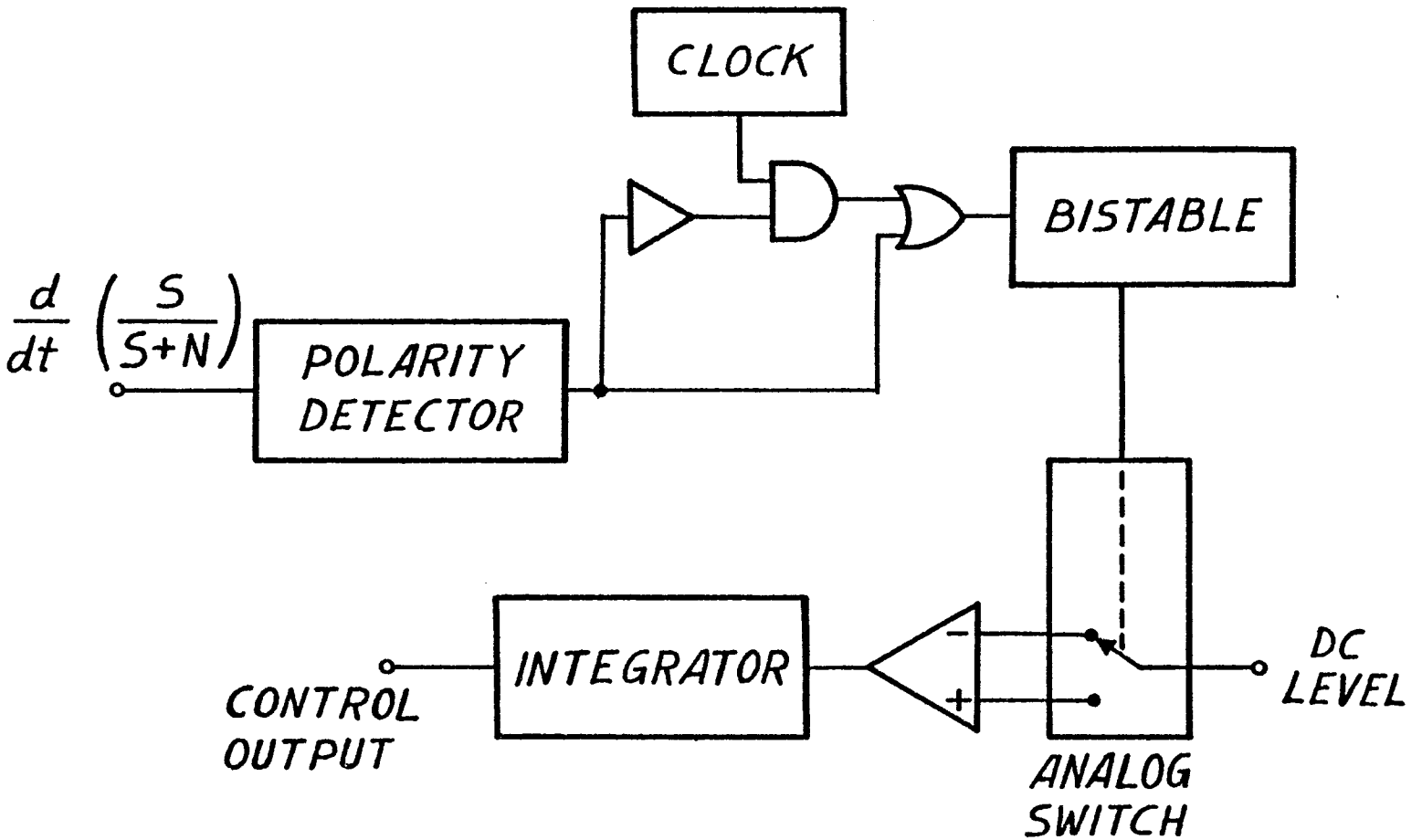


Fig. 16: Schematic diagram for the implementation of the control law.

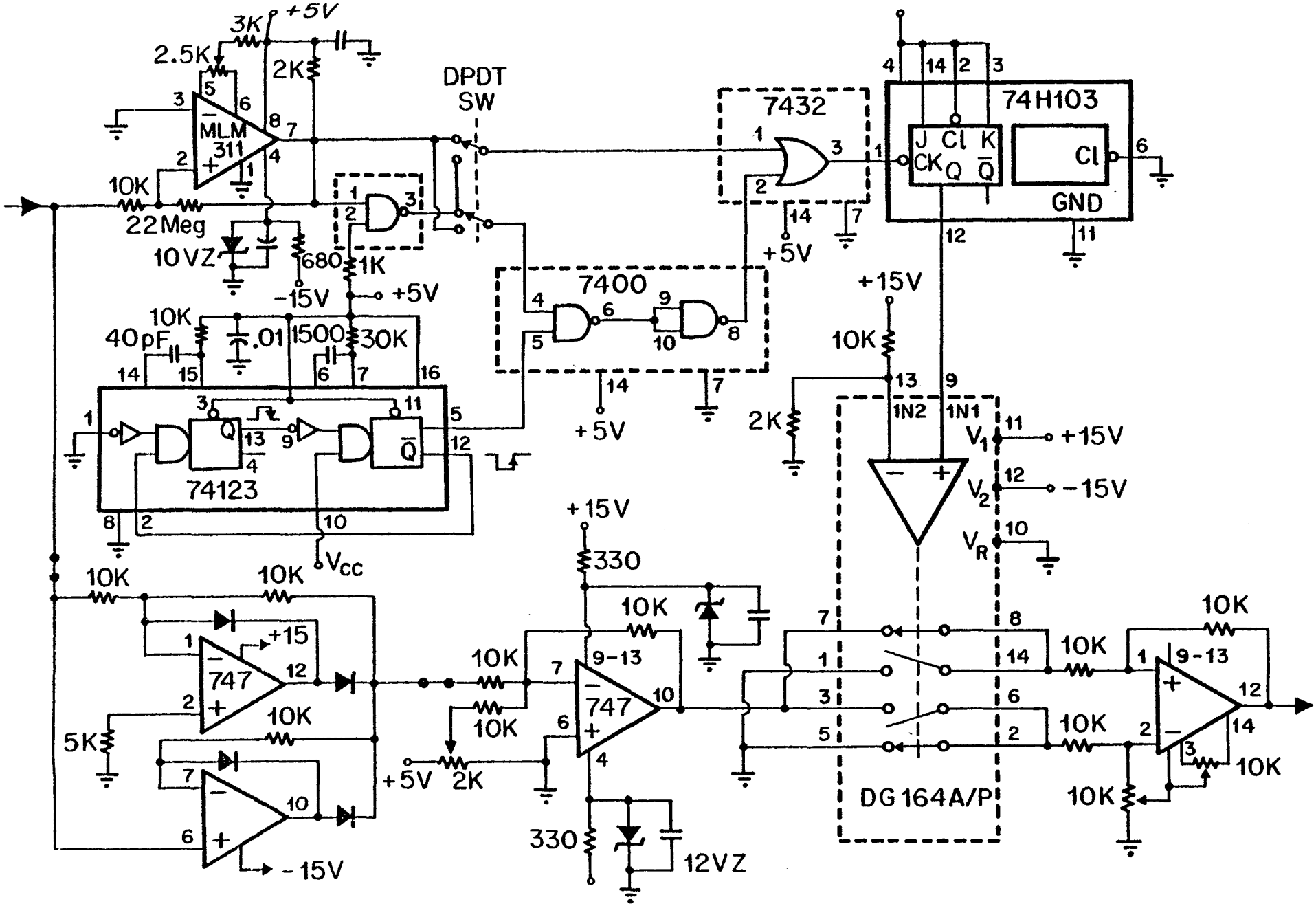


Fig. 17: Experimental realization implementing the control law.

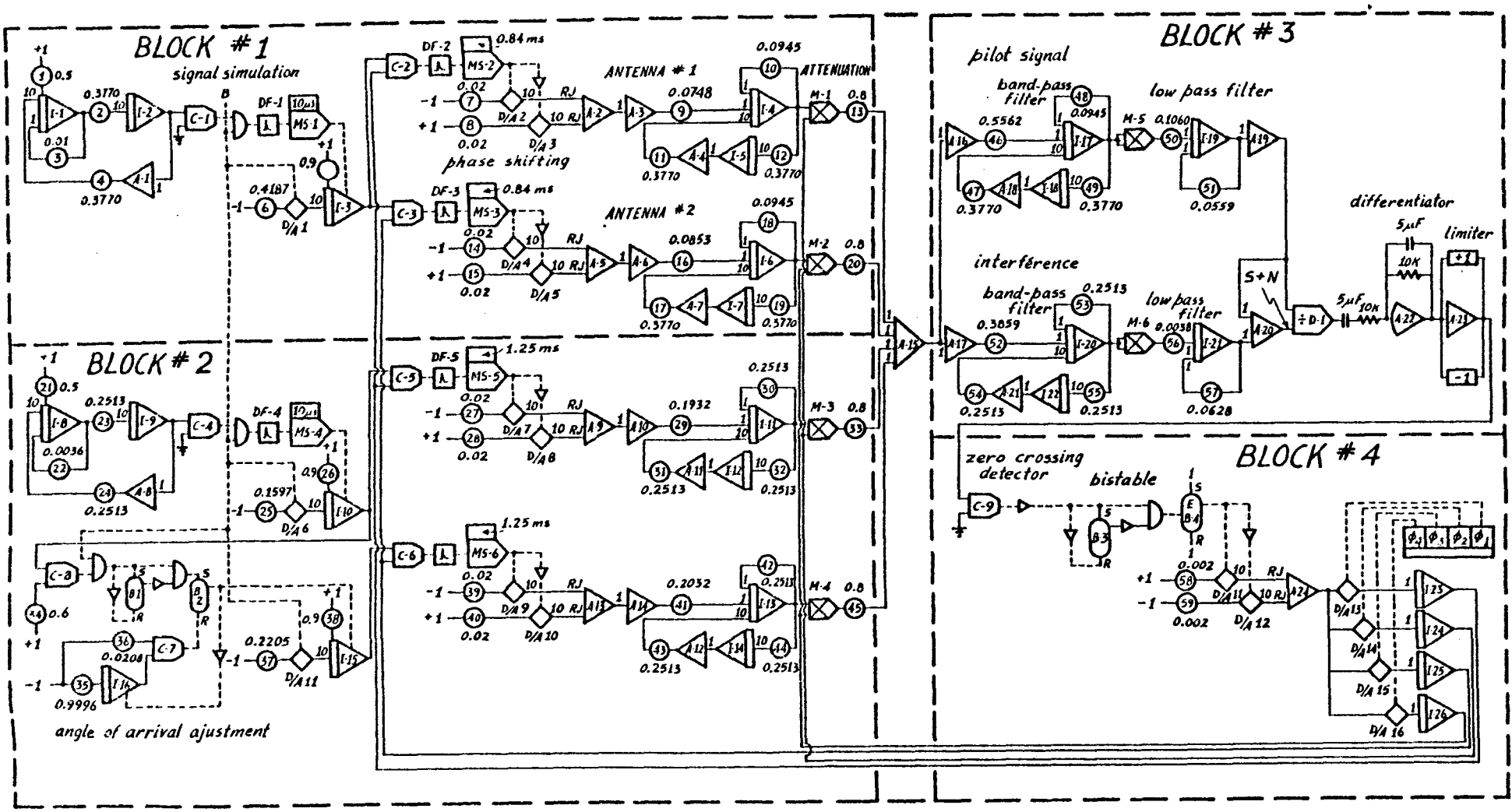


Fig. 18: Diagramme de simulation sur calculateur analogique-digital.

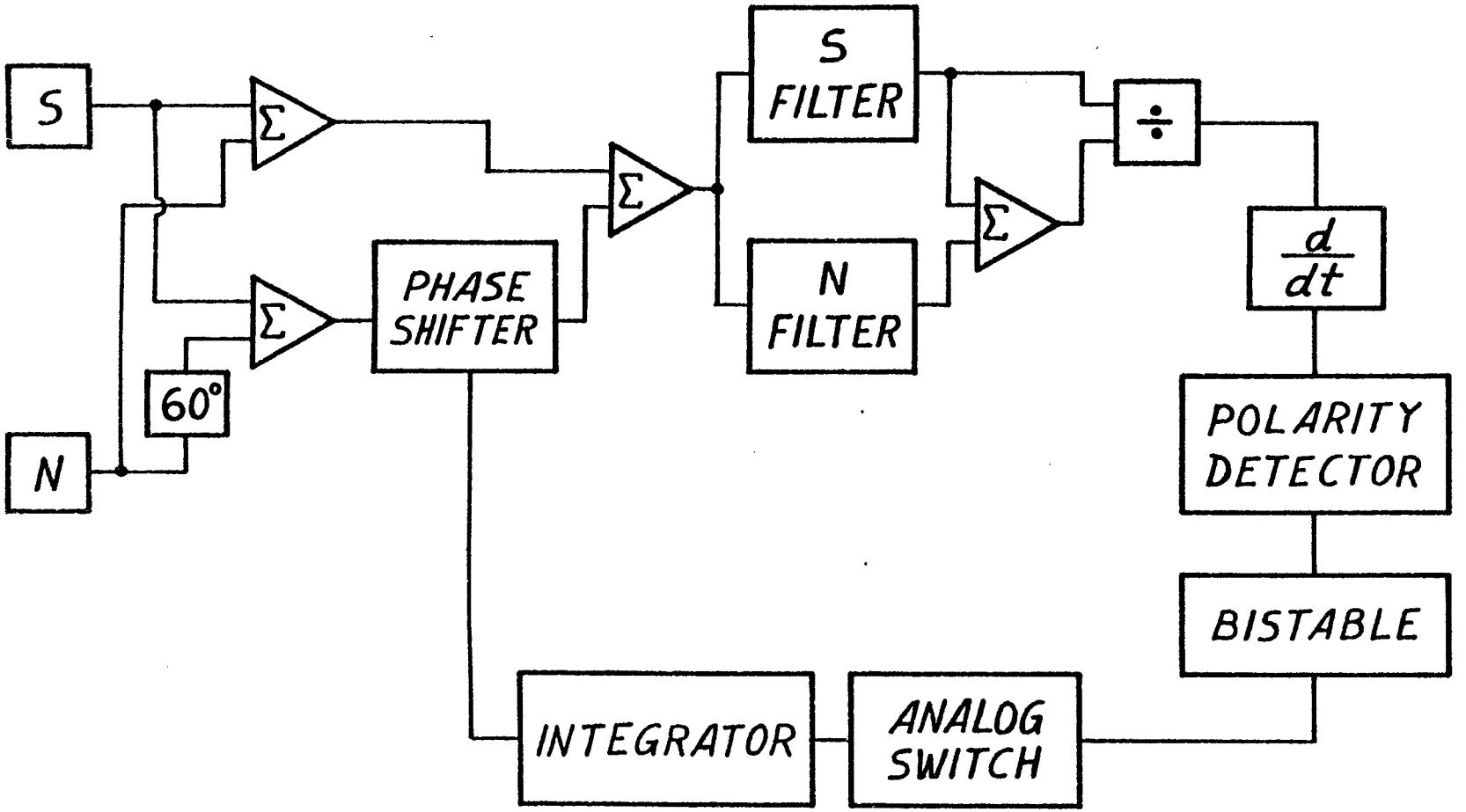


Fig. 19: Représentation schématique de la simulation pour une seule boucle.

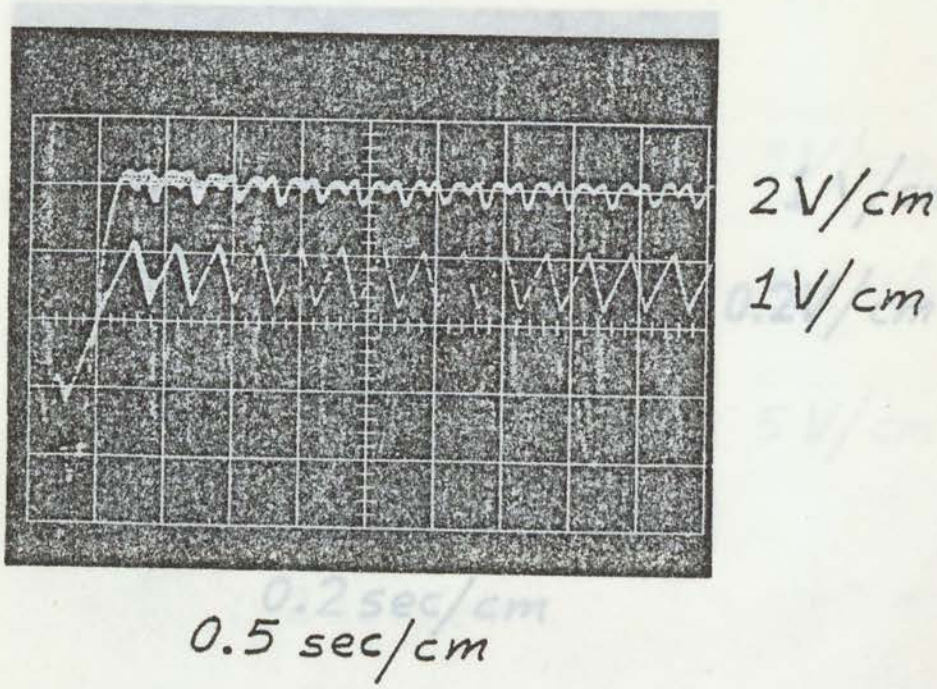


Fig. 20: Courbes de simulation: courbe supérieure: S/(S+N); courbe inférieure: tension de contrôle du déphaseur.

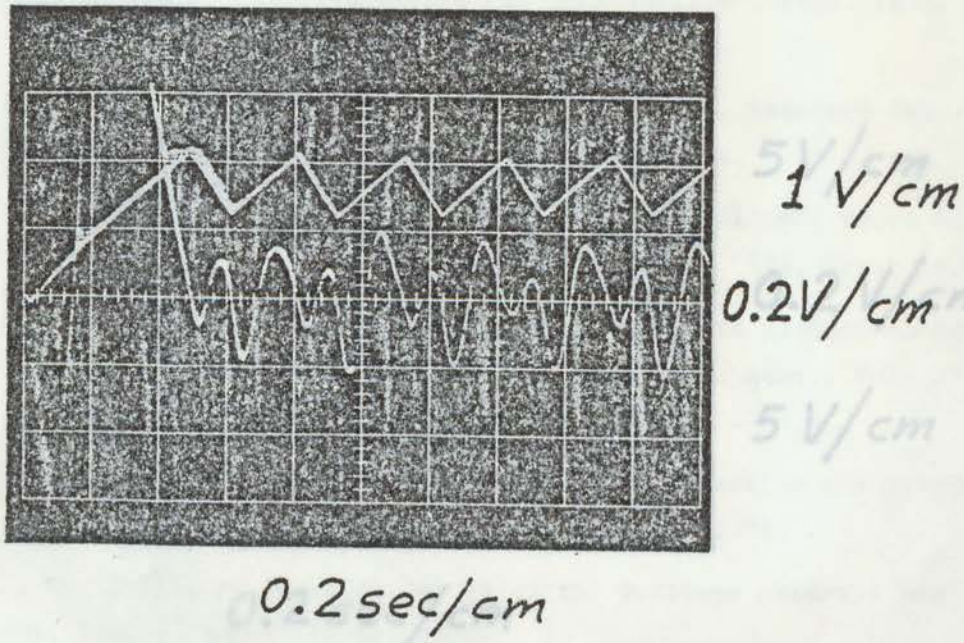


Fig. 21: Courbes de simulation:
courbe supérieure: tension de contrôle du déphaseur;
courbe inférieure: signal de la dérivée de S/(S+N).

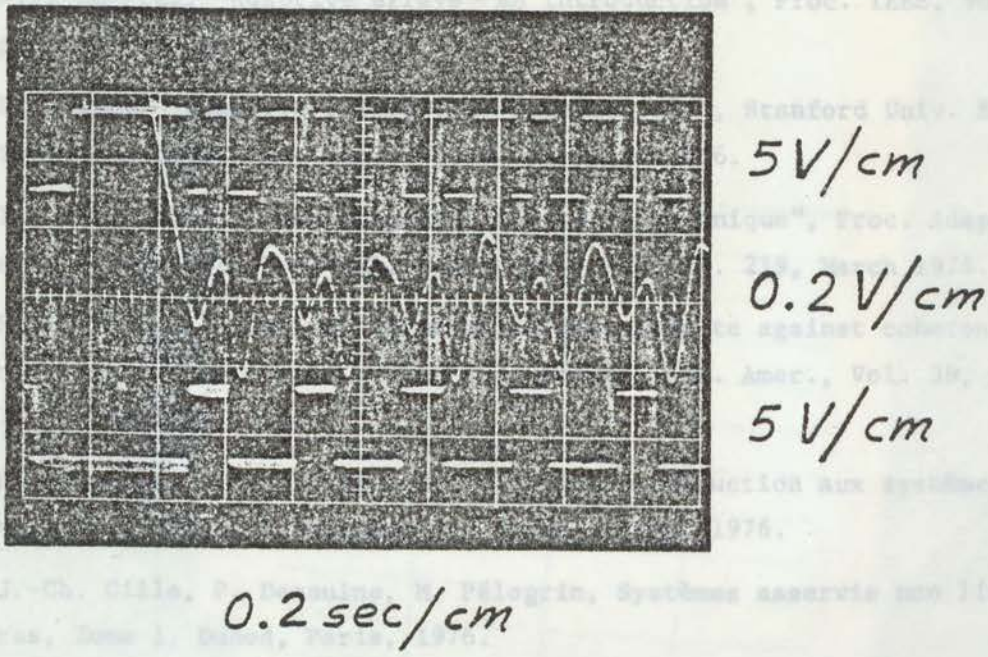


Fig. 22: Courbes de simulation:
courbe supérieure: sortie du détecteur de polarité;
courbe médiane: signal de la dérivée de S/(S+N);
courbe inférieure: sortie du bistable.

## REFERENCES


[1] B. Widrow et al, "Adaptive antenna systems", Proc. IEEE, Vol. 55, pp. 2143-2159, December 1967.

[2] Special Issue on Adaptive Antennas, IEEE Trans. Antennas Propagat., Vol. AP-24, September 1976.

[3] W.F. Gabriel, "Adaptive arrays - an introduction", Proc. IEEE, Vol. 64, pp. 239-272, February 1976.

[4] B. Widrow, "Adaptive filters, I: Fundamentals", Stanford Univ. Electronics Labs., Tech. Rep. 6764-6, December 1966.

[5] I.S. Reed et al, "Sample matrix inversion technique", Proc. Adaptive Ant. System Workshop, NRL, Washington, D.C., p. 219, March 1974.

[6] S.W.W. Shor, "Adaptive technique to discriminate against coherent noise in a narrow-band system", J. Acoust. Soc. Amer., Vol. 39, pp. 74-78, January 1966.

[7] P. Decaulne, J.-Ch. Gille, M. Pélegrin, Introduction aux systèmes asservis extrémaux et adaptatifs, Dunod, Paris, 1976.

[8] J.-Ch. Gille, P. Decaulne, M. Pélegrin, Systèmes asservis non linéaires, Tome 1, Dunod, Paris, 1976.

[9] J.G. Graeme, Applications of operational amplifiers, McGraw-Hill, New York, 1973, p. 78.

[10] R.F. Harrington, Field computation by moment methods, Macmillan, New York, 1968, p. 192.

[11] D.K. Cheng, F.I. Tseng, "Maximization of directive gain for circular and elliptical arrays", Proc. IEE (London), Vol. 114, n° 5, pp. 589-594, May 1967.